NASA Technical Memorandum 81266

Flying-Qualities Criteria for Wings-Level-Turn Maneuvering During an Air-to-Ground Weapon-Delivery Task

Robert I. Sammonds and John W. Bunnell

April 1981

National Aeronautics and
Space Administration

NASA Technical Memorandum 81266

Flying-Qualities Criteria for Wings-Level-Turn Maneuvering During an Air-to-Ground Weapon-Delivery Task

Robert I. Sammonds, Ames Research Center, Moffett Field, California

and

John W. Bunnell, Air Force Flight Dynamics Laboratory, Air Force Wright Aeronautical Laboratories, Wright-Patterson Air Force Base, Ohio

National Aeronautics and
Space Administration

Ames Research Center
Moffett Field, California 94035

TABLE OF CONTENTS

NOMENCLATURE

A	transport delay
AFFDL	Air Force Flight Dynamics Laboratory
AFFTC	Air Force Flight Test Center
AFSC	Air Force Systems Command
ALPHA	angle of attack
A_y,AY	lateral acceleration
A_z,AZ	normal acceleration
a,b	real roots of quadratic equations
b	wing span
C	coarse task
CAS	control augmentation system
CEP	circular error probable
C-H	Cooper-Harper rating scale (see fig. 12)
$\bar{c}$	mean aerodynamic chord
DA	aileron deflection
DCOL	longitudinal stick deflection
DDT	differential tail deflection
DHT	horizontal tail deflection
DLAT	lateral stick deflection
DPED	pedal deflection
DR	rudder deflection
F	fine task or force
FCOL	longitudinal stick force
FLAT	lateral stick force

g	gravity
HUD	head-up display
I_{XX}	roll moment of inertia
I_{XZ}	product of inertia
I_{YY}	pitch moment of inertia
I_{ZZ}	yaw moment of inertia
K_y, K_B, K_{BI}	gains in WLT mechanization
K_Q	gain in basic aircraft control system
ℓ_{acc}	accelerometer location with respect to center of gravity
m	mass
P,PB	roll rate
PIO	pilot-induced oscillation
PR	pilot rating
p	pressure
Q,QB	pitch rate
$\dot{Q}$,QBD	pitch acceleration
R,RB	yaw rate
RBD	yaw acceleration
S	reference wing area
s	Laplace operator, $\frac{d}{dt}$
T_B	time of bomb drop
T_L	time of signal light
T_1	time constant (lead term in transfer function)
t	time
V_T	true airspeed
WLT	wings-level turn

α	angle of attack
β	sideslip angle
γ	dive angle
δ	control or surface deflection
ζ	damping ratio
ρ	air density
τ	equivalent time constant (required for the lateral acceleration response to a unit step input to reach 63.2% of its steady-state value)
ϕ	bank angle
ψ	heading angle
ω	frequency
ω_b	bandwidth frequency
ω_n	natural frequency

Subscripts:

a	aileron
CAL	calibrated
CAS	control augmentation system (electrical)
c.g.	center of gravity
DT	differential tail
HT	horizontal tail
LAT	lateral
LON	longitudinal
Mech	mechanical system
PED	pedal
p	pilot location
R	rudder

ST	stick
s	static
T	total

Coefficients and Stability Derivatives:

C_{ℓ_p}	change in rolling-moment coefficient due to roll rate
C_{ℓ_β}	change in rolling moment coefficient due to sideslip angle
$C_{\ell_{\delta_a}}$	change in rolling-moment coefficient due to aileron deflection
$C_{\ell_{\delta_{DT}}}$	change in rolling-moment coefficient due to differential tail deflection
$C_{\ell_{\delta_R}}$	change in rolling-moment coefficient due to rudder deflection
C_{m_q}	change in pitching-moment coefficient due to pitch rate
$C_{m_{\delta_{HT}}}$	change in pitching-moment coefficient due to horizontal tail deflection
C_n	yawing-moment coefficient
C_{n_r}	change in yawing-moment coefficient due to yaw rate
C_{n_β}	change in yawing-moment coefficient due to sideslip angle
$C_{n_{\delta_a}}$	change in yawing-moment coefficient due to aileron deflection
$C_{n_{\delta_{DT}}}$	change in yawing-moment coefficient due to differential tail deflection
$C_{n_{\delta_R}}$	change in yawing-moment coefficient due to rudder deflection
C_Y	side-force coefficient
C_{Y_β}	change in side-force coefficient due to sideslip angle
$C_{Y_{\delta_R}}$	change in side-force coefficient due to rudder deflection

FLYING-QUALITIES CRITERIA FOR WINGS-LEVEL-TURN MANEUVERING DURING AN AIR-TO-GROUND WEAPON-DELIVERY TASK

Robert I. Sammonds

Ames Research Center

and

John W. Bunnell

Air Force Flight Dynamics Laboratory
Air Force Wright Aeronautical Laboratories
Wright-Patterson Air Force Base, Ohio

SUMMARY

A moving-base simulator experiment conducted at Ames Research Center demonstrated that a wings-level-turn control mode improved flying qualities for air-to-ground weapon delivery compared with those of a conventionally controlled aircraft. Evaluations of criteria for dynamic response for this system have shown that pilot ratings correlate well on the basis of equivalent time constant of the initial response. Ranges of this time constant, as well as digital-system transport delays and lateral-acceleration control authorities that encompassed Level I through III handling qualities, were determined.

INTRODUCTION

Dive bombing is the most common method of delivering free-fall, nonnuclear weapons against ground targets. Compared to the low-level attack mode, it offers the advantages of better target acquisition, reduced vulnerability to certain types of hostile ground fire, and delivery of large-yield low-drag weapons. However, the delivery variables (airspeed, altitude, and attitude) are not as easily attainable as in low-level bombing and the attack is often less accurate. To secure a direct hit, the aircraft must arrive at a particular point in space with the correct airspeed, dive angle, and "g" loading, and with proper corrections made for existing wind conditions.

Motivation for improving the dive-bombing task is threefold: 1) to increase the aiming accuracy; 2) to decrease pilot workload; and 3) to decrease aircraft vulnerability by decreasing the time to acquire the target, aim, and launch the weapon.

Previous investigations (refs. 1-3) have shown that certain advanced control modes can provide a large increase in the combat potential of conventional aircraft because of the control mode's effectiveness in increasing

agility and preciseness of aircraft maneuvers. One of the most promising of these advanced control modes for use in the dive-bombing task (ref. 3) is wings-level turn (WLT). This mode permits a heading change by commanding a lateral acceleration while holding the wings level ($\phi = 0$) and maintaining a zero sideslip ($\beta = 0$). This maneuver eliminates the pendulum motion of the fixed depressed reticle sight (pipper) that occurs during rolling maneuvers when the aircraft's roll axis and the sight do not coincide. Elimination of the pendulum motion allows for a more rapid and accurate acquisition of the target than can be accomplished with a conventional airplane, thus reducing time over the target by permitting increased delivery speeds.

Although existing flight and simulation data show the potential advantages of WLT capability, there is a lack of systematic research on the flying-qualities criteria required for use in design of this control mode. The purpose of the research reported herein was to conduct a systematic, parametric investigation of the variables affecting the performance of an aircraft during an air-to-ground weapon-delivery task using the WLT control mode and to compare these results with those for a conventional, current-generation (bank to turn) fighter aircraft. This program was conducted in Ames Research Center's six-degrees-of-freedom Flight Simulator for Advanced Aircraft (FSAA). Evaluations were obtained for a range of equivalent system dynamic characteristics, digital transport delays, and control authorities. Results are presented in this paper in the form of pilot ratings, commentary, control usage, and time histories.

SIMULATION TEST PROGRAM

Description of Simulator

This investigation was conducted using the six-degrees-of-freedom Flight Simulator for Advanced Aircraft (FSAA) shown in figure 1. This simulator, described in reference 4, was equipped to represent a fighter cockpit with a center stick, all necessary instrumentation (fig. 2, table 1), a head-up display (fig. 3), and hydraulically actuated control loaders on all three axes. The head-up display provided the pilot with a fixed depressed reticle sight, digital readouts of velocity and altitude, a vertical scale to indicate dive angle, bugs to indicate the desired release altitude and airspeed, as well as a conventional pitch ladder. The altitude and airspeed scales located on either side of the display were movable and indicated the rate at which each parameter was varying. The digital readouts of velocity and altitude were updated at varying time rates depending on the rate of change of each variable to make the digital presentation more readable. The control loaders were programmed to give the cockpit control force-feel characteristics typical of an advanced fighter aircraft. The desired and the actual force-feel characteristics obtained are shown in figure 4 for all three axes.

The pilot in the cab was provided visual and aural cues as well as motion cues. The visual cues consisted of a black and white bull's-eye target — located on a terrain board (fig. 5) and displayed on a color TV monitor —

viewed through a collimating lens mounted above the instrument panel. The visual scene was generated by a computer-driven, six-degrees-of-freedom TV camera that duplicated the aircraft motion with respect to the dive-bombing task, but restricted the pilot to a forward view (no side-window viewing capability). Scale-sized buildings were placed near the target to add realism to the scene. The performance capabilities of the visual display system (see VFA-07, table 4.2.1-1 in ref. 4) were modified in the pitch plane by biasing the pitch prism to obtain the necessary look-down capability for the dive-bombing task. The maximum pitch displacements, as used, were +10° to -40°. The downward limitation effectively limited the desired dive angle for the bombing runs to -30°. The aural cues consisted of engine noise modulated by engine rpm and introduced into the cab through stereo speakers.

Modeling

A conventional six-degrees-of-freedom mathematical model was developed to represent a state-of-the-art fighter aircraft. This model was used as the baseline aircraft and had flying qualities similar to those of the F-15. The physical characteristics of this aircraft and the nominal stability derivatives used during the dive-bombing task are presented in tables 2 and 3, respectively. Block diagrams of the pitch, roll, and yaw control systems, including CAS modes, for this basic aircraft are shown in figure 6. Time histories of the aircraft response to longitudinal, lateral, and pedal step inputs are presented in figures 7, 8, and 9, respectively.

The WLT flight-control mode was modeled as a transfer function, relating lateral acceleration to rudder-pedal deflection, of the form

$$\frac{A_y}{\delta_{PED}} = \frac{(K_y/3.25)(T_1 s + 1)e^{-As}}{\frac{s^2}{\omega_n^2} + \frac{2\zeta s}{\omega_n} + 1}$$

The block diagram in figure 10 shows the manner in which the WLT mode was mechanized for the simulation. A proportional-plus-integral sideslip-angle feedback was included to ensure minimal sideslip. The commanded lateral acceleration was introduced directly to the sideforce equation and the calculated yaw rate (including feedback terms) was used directly in the yaw equations of motion. Although this technique did not simulate any real aircraft or aircraft design, it did facilitate the variation of important flying-qualities parameters and allowed the study of pure, uncoupled responses, thus justifying the idealized simulation.

Test Conditions

The gain (K_y), time constant (T_1), transport delay (A), natural frequency (ω_n), and the damping ratio (ζ) of the A_y/δ_{PED} transfer function were subject to variation, either singly or in combination, during the experiment. The primary investigation was to evaluate the effect of the undamped natural

frequency and the damping ratio on handling qualities of the WLT control mode. The matrix for these runs is shown in table 4 for various values of bandwidth (ω_b). Bandwidth is defined as the frequency at which the amplitude of the Bode plot decreases by 3 db from a steady-state condition (see sketch in table 4).

Additional investigations were made to evaluate the effect of adding various amounts of lead (T_1) to an obviously deficient system, various amounts of transport delay (A) to a system having good handling qualities, and three levels of commanded authority (K_y). The matrices for these programs are presented in tables 5 and 6.

Task

The test program was limited to an air-to-ground weapon-delivery task using a fixed depressed-reticle sight and an unguided bomb. The piloting task was to roll onto the target from a 90° heading offset at an altitude of 3,048 m (10,000 ft), establish a -30° dive angle, and release the bomb at a specified set of release conditions (airspeed and altitude). For all runs, the desired release conditions were a dive angle (γ) of -30°, a velocity (V_T) of 365.76 m/sec (1,200 ft/sec), and an altitude of 1,524 m (5,000 ft). The high release velocity was determined from preliminary runs in conjunction with the initial and release altitudes because it resulted in a difficult task — one that could be accomplished with a good system, but could not be accomplished with a poor one. The average time for each run, from target acquisition to bomb drop, was between 4 and 5 sec. A schematic of the dive-bombing task and a sketch of the target is shown in figure 11. Because the visual presentation in the cab did not provide for side-window viewing, the initial heading change and roll-in until target acquisition was an open-loop task that had to be learned by the pilots. They were given sufficient practice time to become proficient at this maneuver.

The bull's-eye target located on the terrain board (see figs. 5 and 11) consisted of concentric circles 50, 100, 500, 1,000, 1,500, and 2,000 ft (scale) in diameter. A normal run was made with respect to the center of the bull's-eye. However, in order to severely exercise the aircraft's WLT capability, a secondary target, a large white dot, was located on the outer ring of the bull's-eye (see fig. 11) normal to the line of flight. Approximately half of the time, in a random manner, a light at the center of the bull's-eye signaled the pilot to bomb the secondary target. This signal was activated only after the pilot was aligned with the primary target, thus necessitating a heading change of about 12° in about 4 sec. Bombing runs to primary and secondary targets will be referred to hereinafter as the fine and coarse tasks, respectively. Although this alternate maneuver probably is not representative of an operational situation, it was selected as a means to subject the WLT mode to a severe heading-change maneuver to evaluate its gross maneuvering capabilities. A similar task could have been induced using wind shears or gusts, but it was felt that the target-change maneuver would generate comparable results.

Data Acquisition

The parametric evaluation of the WLT control mode was accomplished by two USAF pilots (A and B) from the 3246th Test Wing (AFSC), Eglin AFB, and by one pilot (C) from the USAF Test Pilots School, Edwards AFB (see the appendix for pilot resumes). Each pilot made at least two runs at both primary and secondary targets for each set of parameters being evaluated, with the targets being selected in a random manner. Each pilot was allowed to make as many runs as was required for an accurate evaluation of the task. At the end of each set of runs, for a given parameter, the pilots were instructed to give pilot ratings for both the fine and coarse tasks - based on the Cooper-Harper (C-H) rating scale shown in figure 12 — giving reasons for the ratings, as well as comments on flying qualities and ability to accomplish the task. A maximum C-H rating of 7 was established as the worst condition since there was never any danger of losing control of the aircraft.

Pilots A and B were responsible for the parametric evaluations listed in table 4. Each of these pilots went through the matrix at least twice. Additional repetitions were made for points having a spread of more than one pilot rating. Ratings for each pilot were averaged to obtain a single value for each parameter variation for each pilot. Average ratings for the two pilots combined were obtained from averages of each pilot for the configuration. The parameters in the matrix were selected randomly to avoid direct comparison with an adjacent point in the matrix. A baseline WLT condition having a natural frequency (ω_n) of 4.5 and a damping ratio (ζ) of 1.0 was specified and used for all practice and training runs. Pilot comments could then be compared with this baseline WLT configuration. Runs were also made with the conventionally controlled (bank-to-turn) aircraft for comparison.

These same pilots (A and B) were also responsible for evaluation of the matrix shown in table 5; however, because of time limitations, they only went through this matrix once. The third pilot (C), from Edwards AFB, was responsible for the control authority evaluation of table 6.

Pertinent input and response parameters were recorded both on eight-channel Brush recorders and on magnetic tape. Initial and release conditions and bomb scores were recorded at the end of each run; however, CEPs were not calculated from the bomb miss distances because of the small sample size for each condition (2-4 runs).

Table 7 shows the individual pilot ratings for each parameter investigated. Where more than one rating is listed, they are for repeat runs. Pilot ratings presented in the figures are either an average of each pilot's ratings or combinations of the two.

RESULTS AND DISCUSSION

As a prelude to the parametric evaluation of the WLT control mode, several preliminary simulations were conducted to establish the baseline airplane

configuration, the dive-bombing task, and the mechanization of the WLT control mode.

Simulator Validation

Validation of the baseline (bank-to-turn) airplane configuration was based on the subjective assessment of a number of pilots from the Air Force Flight Test Center (AFFTC), Edwards AFB; Air Force Flight Dynamic Laboratory (AFFDL), Wright-Patterson AFB; and Ames Research Center. All were experienced at flying modern fighter aircraft (F-4, F-15, A-7, and T-38) and with air-to-ground weapon delivery. Most were graduates of either the Air Force or the Navy test pilots school. All agreed that the baseline configuration was a good representation of a modern state-of-the-art fighter aircraft with good flying qualities. The F-15 pilots felt it to be comparable to an F-15.

The dive-bombing task was thought to be satisfactory for the evaluation of the WLT control mode, although there were some misgivings due to the lack of side-window viewing. However, the open-loop task of acquiring the target from a 90° heading offset was easily learned. The mechanization of WLT through the rudder pedals was thought to be natural and was readily accepted by all evaluation pilots. The simulator motion provided realistic onsets of the lateral accelerations being commanded, but constraints on the simulator motion restricted the instantaneous lateral accelerations to ±2.4 m/sec^2 (±8.0 ft/sec^2).

Wings-Level Turn

Frequency- The matrix shown in table 4 can be broken down into an evaluation of three underdamped ($\zeta < 1$), two overdamped ($\zeta > 1$), and one critically damped configuration having the following transfer functions:

$$\frac{A_y}{\delta_{PED}} = \frac{K_y/3.25}{\frac{s^2}{\omega_n^2} + \frac{2\zeta s}{\omega_n} + 1} \quad ; \quad \zeta < 1$$

$$\frac{A_y}{\delta_{PED}} = \frac{K_y/3.25}{\left(\frac{s}{\omega_n} + 1\right)^2} \quad ; \quad \zeta = 1$$

$$\frac{A_y}{\delta_{PED}} = \frac{K_y/3.25}{\left(\frac{s}{a} + 1\right)\left(\frac{s}{b} + 1\right)} \quad ; \quad \zeta > 1$$

where a and b are the real roots of the quadratic equation (see table 8).

Figures 13 through 15 show the variation of pilot rating as a function of natural frequency (ω_n) for the three underdamped cases (ζ = 0.3, 0.5, and 0.7). Figures 16 through 18 show this same variation as a function of the low-frequency root (a) for the two overdamped cases (ζ = 1.4 and 2.0). The critically damped case is included in each figure for comparison. Average

pilot ratings are shown in figures 13 and 16 for pilot A, in figures 14 and 17 for pilot B, and in figures 15 and 18 for both together.

All cases show that pilot ratings improve with increasing frequency for a given damping ratio, indicating that increased quickness of response was favorable. This improvement in response is readily discernible in figures 19(a) and (b), which show time histories of pedal displacement and lateral acceleration for frequencies of 1 and 8 rad/sec and a damping ratio of 0.7. For the low-frequency case ($\omega_n = 1.0$) there is considerable lag between pedal input and the lateral acceleration obtained. This response is significantly improved at the higher frequency ($\omega_n = 8.0$). Similar results were obtained for the overdamped cases.

It can also be seen in figures 13 through 15 that there is considerable variation in pilot rating due to the damping ratio (ζ), with the ratings improving with increased damping. Time histories (figs. 20(a) and (b)), typical of this condition, show the improvement in aircraft response because of an increase in the damping ratio, with the frequency being constant. Although the lag between pedal input and A_y response appears similar for the different damping ratios it is obvious that the large overshoots occurring for the lower damping ratio would make it more difficult to put the pipper on the target and hold it there, thus increasing the pilot workload.

Since the high-frequency root (b) in the transfer function for the overdamped cases

$$\left(\frac{A_y}{\delta_{PED}} = \frac{K_y/3.25}{\left(\frac{s}{a} + 1\right)\left(\frac{s}{b} + 1\right)} \right)$$

is generally well separated from the low-frequency root (a), this transfer function can, in most cases, be treated essentially as a first-order system. Figures 16 through 18 show this variation clearly as there are no significant differences in the data obtained for damping ratios of 1.4 and 2.0.

Pilot ratings obtained for the critically damped case are considerably worse than for the overdamped cases and somewhat worse than the best underdamped case ($\zeta = 0.7$) for frequencies less than about 8 rad/sec. Although the reason for the poorer ratings for the critically damped case can probably be discerned from the data presented in tables 4 and 8, further discussion on this matter will be postponed until later in the report (see section on Bandwidth).

In general, pilot comments regarding these data indicate that the ratings are primarily related to the amount of observable lag in the system. The more apparent the lag, the worse the pilot rating. As the lag increases, the system response slows and it becomes more difficult for the pilot to control the inputs without getting overshoots. In extreme cases, the pilot either cannot get the pipper over to the target or cannot stop it, once it is moving, without incurring large overshoots. Although this apparent lag can be attributed to either frequency or damping, the pilots generally seem to prefer quickness (increase in ω_n) to damping, feeling that they can overcome some lack of

damping if the response is quick enough. However, there appears to be a limit to the amount of quickness and damping desired. For extreme cases of high damping and frequency, the pilots complained that the response was jerky and somewhat less than optimum. The very fast starting and stopping of the motion was disorienting. Indications of this degradation are evident in data presented in figures 16 through 18.

Bandwidth- It was hypothesized that the pilot-rating data might better correlate on the basis of the system bandwidth, where bandwidth is defined as the frequency at which there is a 3 db drop in amplitude from the steady-state condition (see table 4). Smooth variations of the average pilot ratings were obtained with this variable for each damping ratio, but there was a definite and distinctive progressive degradation in flying qualities accompanying a decrease in damping. These data are presented in figures 21 through 23. Time histories in figures 24 and 25 show that for a given bandwidth there are significant differences in the time response between pedal input and lateral acceleration as a function of the frequency and damping. Since the same bandwidth can be obtained for various combinations of damping and frequency (see table 4), the higher the frequency and damping for a given bandwidth, the better the pilot rating. It can also be seen from table 4 that the bandwidth decreases with increased damping for a given natural frequency. This variation probably accounts for the poorer ratings shown in figures 13 through 15 for the $\zeta = 1.0$ condition as compared to that for a damping ratio of 0.7. Even though this decrease in bandwidth continues for damping ratios greater than 1, the disparity in the highest frequency roots ($\zeta \geq 1.0$) for systems with the same bandwidth can account for the differences in ratings. Thus, since bandwidth alone cannot be a criterion, phase margin must also be a factor. Preliminary work by Systems Technology, Inc. (ref. 5) has shown correlation of these data on the basis of bandwidth, defined as the lowest frequency for which the open-loop phase margin is at least 45° and the gain margin is at least 6 db. In this definition, the closed-loop system bandwidth is implicitly defined as the open-loop crossover frequency.

Equivalent time constant- Since neither frequency nor bandwidth (as defined in table 4) fully correlates the data, a parameter other than frequency was sought. An evaluation of the pilot comments, recorded during the simulation, showed their concern for the initial time-response characteristics of each configuration on flying qualities. As a result, equivalent time constants were calculated for each test condition listed in table 4. For the overdamped and critically damped cases, the time constant was taken to be the time at which the response to a unit step input reached 63.2% of its steady-state value. For these cases the responses were given by

$$A_y = K_y\left(1 - e^{-\omega_n t} - \omega_n t\, e^{-\omega_n t}\right)$$

for $\zeta = 1$, and

$$A_y = K_y\left(1 + \frac{a\, e^{-bt} - b\, e^{-at}}{b - a}\right)$$

for $\zeta > 1$, where a and b are the real roots of the quadratic equation (table 8). For the underdamped oscillatory response, time constant was based on the envelope of the response as calculated by

$$A_y = K_y\left(1 - e^{-\zeta\omega_n t}\right)$$

This time constant was equivalent to the time to damp to 36.8% of the initial amplitude.

Pilot ratings in figures 26 through 28, presented as a function of these equivalent time constants, show excellent correlation for all data, both fine and coarse tasks. It should be pointed out that pilot ratings for both tasks are nearly the same, differing by only about half a rating. Time constants and average pilot ratings for the two pilots are shown in table 9.

These data show that there is a minimum equivalent time constant (0.15-0.2 sec) at which optimum performance of WLT is achieved. Level I performance (C-H $\leq$ 3.5) was obtained for time constants less than about 0.4 sec for the fine task and less than about 0.35 sec for the coarse task. The WLT ratings became unacceptable at time constants greater than about 1.5 sec. These results agree with pilot comments that the lag of the system was the most important factor determining their ratings. As previously mentioned, the pilots felt they could tolerate some lack of damping if the response was quick enough; but if it was too quick, performance became jerky and disorienting and flying qualities deteriorated somewhat. The slight break in the curves (figs. 26 to 28) at the low time constants is indicative of this deterioration.

The distribution of all pilot ratings for pilots A and B (table 7) are shown in figure 29 for both fine and coarse tasks as a function of the equivalent time constant. The symbol legend denotes number of times each rating was repeated. These data show a band of approximately ± 1 pilot rating for each time constant. This is indicative of the repeatability of ratings and the validity of results in figure 28.

Time histories — showing the effect of pedal input on lateral acceleration response as a function of the equivalent time constant — are presented in figures 30 and 31 for underdamped and overdamped cases, respectively. Although the time constant in these figures is a function of ω_n and a constant damping ratio, the data are directly comparable on the basis of the time constant without regard to either the damping ratio or frequency stipulated. These data show that the system's response quickens with decreasing equivalent time constants.

The equivalent time constant is effective as a correlating parameter for these data. Apparently this is because it directly represents the time lag for the overdamped cases as well as the time to damp to some percentage of the initial amplitude for the underdamped cases (particularly those with low damping).

Lead and Transport Delay

Tests were conducted to examine the effect of adding lead to an obviously deficient system and of adding transport delay to a previously good system (figs. 32 and 33, respectively). Figure 32 shows the average pilot ratings as a function of the lead time constant for the transfer function

$$\frac{A_y}{\delta_{PED}} = \frac{(K_y/3.25)(T_l s + 1)}{\frac{s^2}{\omega_n^2} + \frac{2\zeta s}{\omega_n} + 1}$$

where $\zeta = 1.0$, $\omega_n = 4.5$. These data show that adding small amounts of lead was beneficial, but that too much ($T_l = 0.6$) became degrading. A $T_l = 0.3$ resulted in fast response with essentially no overshoot and the best pilot rating of any system tested, whereas a $T_l = 0.6$ resulted in jerky response and a discernible degradation in the rating. Time histories for lead time constants of 0 and 0.3 sec (fig. 34) clearly show improvement in system response due to addition of the 0.3 sec lead term to the transfer function. Unfortunately, data showing system response to addition of the 0.6 sec lead was not recoverable from the magnetic tape.

The effect of adding a transport delay to a good system is shown in figure 33 for the transfer function

$$\frac{A_y}{\delta_{PED}} = \frac{(K_y/3.25)e^{-As}}{\left(\frac{s}{a} + 1\right)\left(\frac{s}{b} + 1\right)}$$

where $\zeta = 1.4$, $\omega_n = 15$, $a = 6.30$, and $b = 35.70$. These data show that adding even small amounts of delay resulted in degraded performance as noted by the increase in C-H ratings with increased delay. Time histories of these responses (fig. 35) show this clearly. This agrees with previous findings that the more lag or delay in a system the more difficult the tracking task becomes. Unfortunately, time histories for the 0.49 sec transport delay were not recoverable from the magnetic tape.

Equivalent time constants calculated for both lead terms and transport delays (table 10) are plotted in figure 36, superimposed on the data band of figure 28. The time constants obtained using various amounts of lead agree well with the data trend established in figure 28 for both fine and coarse tasks. These data clearly show the degradation in performance for systems that are too quick ($T_l = 0.6$, $\tau = 0.07$) and further emphasizes that there is some minimum equivalent time constant for optimum performance.

The equivalent time constants calculated for various transport delays ($\tau_{basic} + A$) are also in relatively good agreement with the basic data except for the transport delay of 0.49 sec ($\tau = 0.68$). Both pilots rated this system unacceptable (C-H = 7) because of large overshoots and PIOs for both fine and coarse tasks. This poor rating is almost certainly a result of low stability margin contributed by the time delay. Although both phase and gain margins are positive for this case, the phase margin is marginal for good

stability. Then, with the addition of the pilot's own time delay, the system's stability degenerates further with the resulting large overshoots and PIOs. The pilot rating shown for a delay of 0.105 sec (τ = 0.29) for the coarse task also appears to be in disagreement with the basic data. This data point, however, is influenced by a C-H rating by pilot A that appears to be poorer than would be expected from figures 33(a) and 35(b). Pilot B's rating would make this data point fall more in line with the basic data.

Control Authority

During an earlier simulation, an investigation was conducted to evaluate the authority required for WLT maneuvering during the air-to-ground weapon-delivery task. Three levels of maximum commanded side acceleration were provided (0.5, 0.75, and 3.0 g). The authorities of 0.5 and 0.75 g's were selected as reasonable or desirable for a control mode of this kind, whereas 3.0 g was selected as sort of an open-ended value so the actual acceleration being used could be determined.

The control system was mechanized to give full pedal travel for each of these authorities (see table 4). Results of these tests are in figure 37, where each curve is a cumulative frequency distribution of the lateral accelerations used during the coarse task maneuver for a configuration having an equivalent time constant of 0.71.

These cumulative distributions were calculated from the commanded lateral accelerations used over a designated time interval for increments of time equal to 0.001 sec. The designated time interval was taken as the time between the minimum side acceleration, occurring after the target change signal was initiated, until the time of the bomb drop. This time interval relates to the time the A_y input was effective in creating a heading change and differs from the time of pedal input due to lag in the A_y response. Typical time histories showing the relationship of the pedal input and A_y response for each of the three control authorities are presented in figure 38.

The curves in figure 37 show the probability of exceeding given levels of authority for each of the three authorities selected. The lowest level of authority (0.5 g) proved inadequate for either the fine or coarse task. Even though the maximum authority of 0.5 g was used nearly 50% of the time, the pilot could produce a heading change that was only about half of that required (coarse task) to complete the task of acquiring the target before passing the release altitude of 1,524 m (5,000 ft). Figure 38(a) shows the time history for this case. Full pedal input was reached in about 1 sec after the signal for a target change, but the full side acceleration of 0.5 g was not obtained for another 1.5 sec because of lag in the system.

For an authority of 0.75 g, pilots still could not translate the pipper through a heading change sufficient to acquire the target in the time allotted to complete the task. It was possible, however, to accomplish the fine task with this amount of authority. Figure 38(b) shows the time history for this case.

With an authority of 3.0 g, the pipper could easily be translated to the target without using the full limit of authority. The time history of this maneuver (fig. 38(c)) shows that a maximum lateral acceleration of 2.5 g was used, but only momentarily. Figure 37 shows that for 50% of the time the probability is that no more than 1 g will be required. The time history data also show that the heading change was completed in sufficient time to do some fine tracking on the target, as evidenced by the oscillatory nature of the pedal input. However, the lag in this particular configuration prevents lateral acceleration from following rapid changes in pedal input. A quicker system would have shown a closer correspondence between pedal input and side acceleration (see fig. 34(b)).

It becomes readily apparent from the data in figures 37 and 38 that the authority required to accomplish the desired heading change to acquire the target is dependent on the equivalent time constant (τ) of the system being investigated. The control power and time response required to make a particular heading change, based on the second-order model used in this investigation, can be seen graphically in figure 39 for a time interval of 5 sec and a release velocity of 710 knots. Since the heading change required for this task was about 12°, authorities of 0.5 and 0.75 g's for a system having an equivalent time constant of 0.71 sec were clearly inadequate for the task. An authority of 3 g would have been adequate even for a marginally acceptable configuration with τ = 1.5 sec. Figure 39 shows that the time constant (τ) significantly affects the authority required. This figure can also be used to estimate control authority and time-response requirements for incremental heading changes and time durations that differ from the particular task investigated in this experiment.

Comparison With Conventional Airplane

Pilots A and B, who evaluated the WLT control mode, also evaluated the conventionally configured (bank-to-turn) airplane for both fine and coarse tasks for the same release conditions — an altitude of 1,524 m (5,000 ft), a dive angle of -30°, and a release velocity (V_T) of 365.76 m/sec (1,200 ft/sec). Individual pilot ratings (table 7) for the coarse task were in close agreement, and the task was rated as being essentially impossible to accomplish (C-H = 6-7). Although this basic aircraft had flying qualities similar to the F-15, it was nearly impossible to bank the airplane, make the necessary heading change, and level out on the target in the time allotted for the task due to both the control authority of the aircraft and the pendulum effect of the pipper. These results for the conventionally configured aircraft illuminate the benefits of WLT for it was shown that the task was easily accomplished when using WLT with good response characteristics ($\tau \approx 0.15$-0.2). One should remember that the task was made particularly difficult so that advantages or disadvantages of different control modes and parametric variations would become obvious.

Pilot ratings for the fine task varied from 3 to 5 (table 7) and depended largely on the ability or luck of the pilot being able to roll out onto the target with the pipper properly aligned. Normally, if more than one bank

maneuver was required to compensate for the pendulum effect of the pipper, the task became very difficult. Pilot A felt the task was difficult but could be done easily with the right guesswork as to the amount of bank modulation needed to overcome the pipper's pendulum effect. He gave this task a rating of 5. Pilot B described the aircraft's damping and control sensitivity as "nice" and said that he could accomplish the task with a minimum of compensation. He gave this task a rating of 3.

It was the general feeling of pilots A and B that WLT with good response characteristics was a significant improvement over the basic aircraft for the air-to-ground weapon-delivery task. WLT greatly simplified the lateral tracking task and allowed more attention to be devoted to the longitudinal task, in comparison with the basic aircraft.

CONCLUDING REMARKS

Piloted six-degrees-of-freedom motion simulator investigations at Ames Research Center demonstrated that the WLT control mode was very useful 1) in decreasing pilot workload during an air-to-ground weapon-delivery task, and 2) in improving airplane flying qualities in comparison with those of a conventional aircraft, particularly if any significant amount of heading change was required to acquire the target.

The parametric evaluation of frequency and damping requirements for the WLT control mode showed that pilot ratings for various combinations of damping ratio and frequency response correlate extremely well on the basis of time required for lateral acceleration response to a unit step input to reach 63.2% of its steady-state value. This equivalent time constant correlated the data for underdamped, overdamped, or critically damped responses.

The data show improved pilot ratings with decreased time constant (response is quickened), but there is a minimum time constant ($\tau \approx 0.15$ sec) for optimum performance. A further decrease in the time constant results in excessive quickness that degrades ratings because of jerkiness and pilot disorientation. In general, equivalert time constants less than about 0.4 sec resulted in pilot ratings of 3.5 or better for both fine and coarse tasks.

The effect of adding lead to the basic transfer function can be interpreted in terms of the equivalent time constant, with these corresponding to the ones obtained from the frequency and damping variations. Any addition of a transport delay to a basically good system degraded the performance and increased the pilot ratings (i.e., made them worse). Most pilot comments regarding degradation in performance pertained to various amounts of transport delay or lag in the system. Only for cases having low damping and low-frequency response did oscillatory motion become a problem. For cases having either high damping and high-frequency response or excessive amounts of lead the problem became one of excessive quickness.

The variation in control authority of 0.5, 0.75, and 3.0 g for a configuration having an equivalent time constant of 0.71 sec showed that both the lower authorities were inadequate to accomplish an abrupt target acquisition task and that 0.5 g was even inadequate for precise target tracking. For the highest authority (3.0 g) a maximum of 2.5 g was used, but only momentarily. For 75% of the time there was a probability that one would not exceed 2 g, and for 50% of the time the probability one would not exceed 1 g. Since the control authority required is also dependent on the equivalent time constant, a quicker response time (smaller time constant) would lead to a lower control authority necessary to accomplish the heading-change maneuver.

APPENDIX

Pilot Resumes

This section contains brief resumes of experience and qualifications of the pilots taking part in this investigation.

Pilot A

Position: Test pilot, USAF/Eglin AFB
Flight time: (h)

Single engine	176
Multiengine	2801
Other	56
Total	3033

Ratings: Single- and multiengine ratings
Instrument rating
Commercial pilot certificate
Airplanes: RF-4C, F-4C, T-38, A-7D, T-37

Pilot B

Position: Test pilot, USAF/Eglin AFB
Flight time: (h)

Single engine	180
Multiengine	1750
Other	50
Total	1980

Ratings: Single- and multiengine ratings
Instrument rating
Airplanes: F-4, T-38, T-37, A-7

Pilot C

Position: Instructor, USAF Test Pilot School/Edwards AFB
Flight time: (h)

Single engine	230
Multiengine	1360
Other	--
Total	1590

Ratings: Single- and multiengine ratings
Instrument rating
Airplanes: F-100, F-4, A-7, A-37

REFERENCES

1. Carlson, E. F.: Direct Sideforce Control for Improved Weapon Delivery Accuracy. AIAA Paper 74-70, Washington, D.C., 1974.

2. Swortzel, Frank R.; and Barfield, Finley A.: The CCV Fighter Program — Demonstrating New Control Methods for Tactical Aircraft. AIAA Paper 76-889, Dallas, Texas, 1976.

3. Brulle, Robert V.; Moran, William A.; and Marsh, Richard G.: Direct Side Force Control Criteria for Dive Bombing. AFFDL-TR-76-78, Vols. I and II, Sept. 1976.

4. Sinacori, John B.; Stapleford, Robert L.; Jewell, Wayne F.; and Lehman, John M.: Researcher's Guide to NASA-Ames Flight Simulator for Advanced Aircraft (FSAA). NASA CR-2875, 1977.

5. Hoh, Roger H.; Myers, Thomas T.; Ashkenas, Irving L.; and Ringland, Robert F.: Development of Handling Quality Criteria for Aircraft with Independent Control of Six Degrees of Freedom. Proposed AFWAL technical report (Systems Technology, Inc.), Wright-Patterson AFB, Ohio (in press).

TABLE 1.- COCKPIT INSTRUMENTATION

Attitude indicator, 2 axis
Horizontal situation indicator
Angle of attack indicator
Altimeter
Instantaneous vertical speed indicator
Normal acceleration, g units
Engine rpm
Indicated airspeed, knots
Mach number
Speed brake position indicator
Longitudinal acceleration, g units
Turn/bank indicator
Sideslip angle indicator
Lateral acceleration, g units
Clock

TABLE 2.- AIRCRAFT PHYSICAL CHARACTERISTICS

Gross weight	15,843 kg (34,928 lb)
Reference wing area (S)	56.49 m^2 (608 ft^2)
Mean aerodynamic chord ($\bar{c}$)	4.88 m (16.00 ft)
Wing span (b)	13.02 m (42.70 ft)
Center of gravity location	26.5% $\bar{c}$
Roll moment of inertia (I_{XX})	34,264 kg-m^2 (25,270 slug-ft^2)
Pitch moment of inertia (I_{YY})	211,114 kg-m^2 (155,700 slug-ft^2)
Yaw moment of inertia (I_{ZZ})	237,960 kg-m^2 (175,500 slug-ft^2)
Product of inertia (I_{XZ})	-1,091 kg-m^2 (-805 slug-ft^2)
Engines (2)	P&W F-100-PW-100

TABLE 3.- STABILITY DERIVATIVES
(M = 1.09, α = 0.75°, and Alt. = 5000 ft)

C_{ℓ_p}	-0.263	C_{n_β}	0.031
C_{ℓ_β}	-.0025	$C_{n_{\delta_a}}$	.00005
$C_{\ell_{\delta_a}}$	.00044	$C_{n_{\delta_{DT}}}$	.000287
$C_{\ell_{\delta_{DT}}}$	.00065	$C_{n_{\delta_R}}$	-.0016
$C_{\ell_{\delta_R}}$	.000056	C_{Y_β}	-.017
C_{n_r}	-.30	$C_{Y_{\delta_R}}$	.0023

TABLE 4.- TEST MATRIX — TRANSFER FUNCTION
Bandwidth for Combinations of Frequency and Damping Ratio

ω_n \ ζ	0.3	.5	.7	1.0	1.4	2.0
0.5	0.71[a]	0.64				
1	1.42	1.27	1.01	0.64	0.41	0.27
2	2.84	2.54	2.02	1.29	.82	.53
3	4.26	3.81	3.03	1.93	1.22	.80
4.5	6.39	5.72	4.55	2.90	1.84	1.20
6			6.06	3.86	2.45	1.60
8			8.08	5.15	3.26	2.13
10				6.44	4.08	2.67
12				7.72	4.90	3.20
15					6.12	4.00
19					7.75	5.07
23						6.13
28						7.46

[a]Bandwidth frequency.

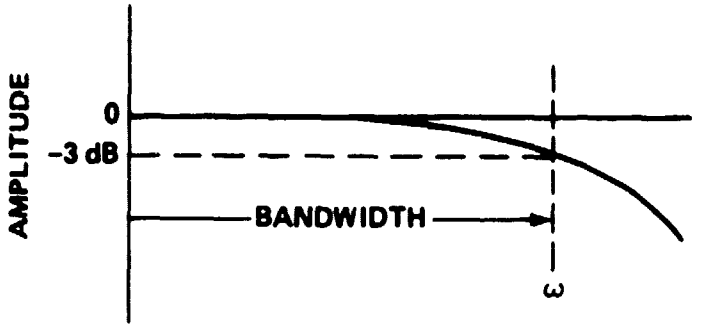

TABLE 5.- TEST MATRIX — LEAD AND TRANSPORT DELAY

$$\frac{A_y}{\delta_{PED}} = \frac{(K_y/3.25)(T_1 s + 1)e^{-As}}{\frac{s^2}{\omega_n^2} + \frac{2\zeta s}{\omega_n} + 1}$$

ω_n	ζ	T_1	A
4.5	1.0	0	--
4.5	1.0	.1	--
4.5	1.0	.3	--
4.5	1.0	.6	--
15	1.4	--	0
15	1.4	--	.105
15	1.4	--	.24
15	1.4	--	.49

TABLE 6.- TEST MATRIX — CONTROL AUTHORITY

$$\frac{A_y}{\delta_{PED}} = \frac{K_y/3.25}{\frac{s^2}{\omega_n^2} + \frac{2\zeta s}{\omega_n} + 1}$$

ω_n	ζ	K_y
2	0.7	3.0
2	.7	.75
2	.7	.50

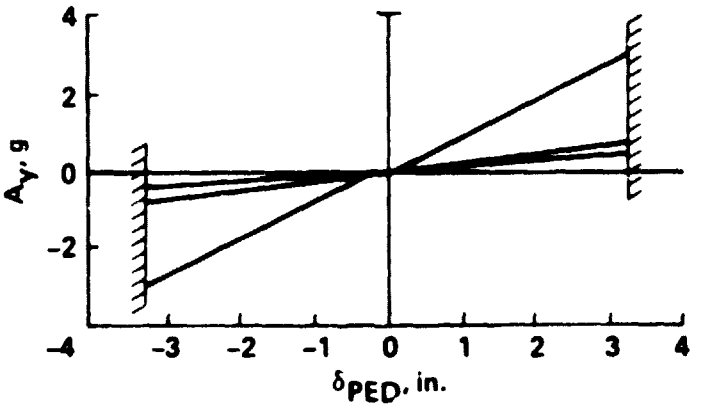

TABLE 7.- PILOT RATINGS AND AVERAGES – (C/F)

(a) $\zeta - \omega_n$ Matrix

ζ	0.3		0.5		0.7		1.0		1.4		2.0	
ω_n	A	B	A	B	A	B	A	B	A	B	A	B
0.5	7/7 7/7	7/7 7/7	7/7 7/7	7/7 7/7								
Avg	7/7	7/7	7/7	7/7								
1	7/7 7/7	7/6 7/7	6/6	7/6 7/7	7/7 7/6	7/7 7/7	7/7 7/7	7/7 7/7	7/7 7/7	7/7 7/7	7/6 7/7	7/7 7/7
Avg	7/7	7/6.5	6/6	7/6.5	7/6.5	7/7	7/7	7/7	7/7	7/7	7/6.5	7/7
2	6/5 7/7	7/6 7/7	7/5 7/7	5/5 5/5	5/6 7/5 7/6	6/5.5 6/5	6/5 7/5	7/7 6/5 6/5	6/6 7/7	7/6 7/7	6/6 7/7	7/7 7/6
Avg	6.5/6	7/6.5	7/6	5/5	6.3/5.7	6/5.3	6.5/5	6.3/517	6.5/6.5	7/6.5	6.5/6.3	7/6.5
3	7/6 7/6	5/5 4/4	6/5 7/5	5/4 4.5/4	6/5 5/4 5/4	4/4 4.5/4	5/5 6/5	4/4.5 5/5	5/5 6/5	5/5 5/5	6/5 7/7	5.5/5 6/5
Avg	7/6	4.5/4.5	6.5/5	4.8/4	5.3/4.3	4.3/4	5.5/5	4.5/4.8	5.5/5	5/5	6.5/6	5.8/5
4.5	4/5 6/6	7/6 6/4.5	4/4 5/5	3/3 4/3	4/3 5/4 4/3	4/3 4.5/3	3/3 5/4 5/5	4.5/4 5.5/4	5/4 4/4	7/6 4/3 5/4	5/5 6/5	6/5 5/5
Avg	5/5.5	6.5/5.3	4.5/4.5	3.5/3	4.3/3.3	4.3/3	4.3/4	5/4	4.5/4	5.3/4.3	5.5/5	5.5/5
6					3/3 2/2	4/3 3/2.5	4/3 3/2	3/3 5/4 4/3	4/4 4/4	5/4.5 4/4	4/4 5/4	5/4 6/5
Avg					2.5/2.5	3.5/2.8	3.5/2.5	4/3.3	4/4	4.5/4.3	4.5/4	5.5/4.5
8					2/2 3/3	4/4 4/2.5 2/2 2.5/2	2/2 2/2	4.5/3.5 3.5/3.5	3/3 4/4	5/4.5 4/4	5/5 5/4	4.5/4.5 4/3
Avg					2.5/2.5	3.1/4.6	2/2	4/3.5	3.5/3.5	4.5/4.3	5/4.5	4.3/3.8
10							3/2 2/2	3/4 2.5/2 2/2	2/2 2/2	5/4.5 4/3 2.5/2	2/2 3/3	4.5/4 4/4
Avg							2.5/2	2.5/2.7	2/2	3.8/3.2	2.5/2.5	4.3/4

TABLE 7.- Continued.

(a) ζ - ω_n Matrix

ζ	0.3		0.5		0.7		1.0		1.4		2.0	
ω_n	A	B	A	B	A	B	A	B	A	B	A	B
12							3/2 2/2	3.5/3.5 2.5/2	3/3 2/2	4/2.5 3/3 2.5/2	2/2 4/3 3/3	3/3 3/3
Avg							2.5/2	3/2.8	2.5/2.5	3.2/2.5	3/2.7	3/3
15									2/2 2/2	2.5/2.5 3/2.5	4/3 2/2 3/3	2/2 4/3 4/4
Avg									2/2	2.8/2.5	3/2.7	3.3/3
19									2/2 3/2	3/3 3/2 5	3/3 2/2	4/3 2/2 3/3
Avg									2.5/2	3/2.8	2.5/2.5	3/2.7
23											3/3 2/2	3/3 3/2
Avg											2.5/2.5	3/2.5
28											3/3 2/2	4/4 3/2.5 2.5/2
Avg											2.5/2.5	3.2/2.8

TABLE 7.- Concluded.

(b) Transport delay, A					
ω_n	ζ	A	τ	Pilot A	Pilot B
15	1.4	0	0.19	2/2	2.8/2.5
15	1.4	0.105	.29	5/3	4/3
15	1.4	.24	.43	5/3	4.5/3.5
15	1.4	.49	.68	7/7	7/7
(c) Lead time constant, T_1					
ω_n	ζ	T_1	τ	Pilot A	Pilot B
4.5	1.0	0	0.48	4.3/4	5/4
4.5	1.0	0.1	.37	2/2	5/4
4.5	1.0	.3	.16	2/2	2/2
4.5	1.0	.6	.07	4/3	3/3
(d) Basic airplane					
Pilot		Coarse		Fine	
A		7		5	
B		6		3	

TABLE 8.- REAL ROOTS OF QUADRATIC DENOMINATOR
$[(s + a)(s + b) = s^2 + 2\zeta\omega_n s + \omega_n{}^2]$

ω_n	ζ	a	b	ζ	a	b
1	1.4	0.42	2.38	2.0	0.27	3.73
2		.84	4.76		.54	7.46
3		1.26	7.14		.80	11.20
4.5		1.89	10.71		1.21	16.79
6		2.52	14.28		1.61	22.39
8		3.36	19.04		2.14	29.86
10		4.20	23.80		2.68	37.32
12		5.04	28.56		3.22	44.79
15		6.30	35.70		4.02	55.98
19		7.98	45.22		5.09	70.91
23					6.16	85.84
28					7.50	104.50

TABLE 9.- EQUIVALENT TIME CONSTANTS AND AVERAGE PILOT RATINGS

ζ / ω_n	0.3			0.5			0.7			1.0			1.4			2.0		
	τ	C	F	τ	C	F	τ	C	F	τ	C	F	τ	C	F	τ	C	F
0.5	6.67	7	7	4.00	7	7												
1	3.33	7	6.8	2.00	6.5	6.3	1.43	7	6.8	2.15	7	7	2.84	7	7	3.98	7	6.8
2	1.67	6.8	6.3	1.00	6	5.5	.71	6.2	5.5	1.07	6.4	5.4	1.42	6.8	6.5	1.99	6.8	6.5
3	1.11	5.8	5.3	.67	5.7	4.5	.48	4.8	4.2	.72	5	4.9	.95	5.3	5	1.33	6.2	5.5
4.5	.74	5.8	5.4	.44	4	3.8	.32	4.3	3.2	.48	4.7	4	.63	4.9	4.2	.88	5.5	5
6							.24	3	2.7	.36	3.8	2.9	.47	4.3	4.2	.66	5	4.3
8							.18	2.8	2.6	.27	3	2.8	.36	4	3.9	.50	4.7	4.2
10										.21	2.5	2.4	.28	2.9	2.6	.40	3.4	3.3
12										.18	2.8	2.4	.24	2.9	2.5	.33	3	2.9
15													.19	2.4	2.3	.27	3.2	2.9
19													.15	2.8	2.4	.21	2.8	2.6
23																.17	2.8	2.5
28																.14	2.9	2.7

TABLE 10.- TIME CONSTANTS AND AVERAGE PILOT RATINGS FOR LEADS AND TRANSPORT DELAYS

(a) Lead (T_l)				
ω_n	ζ	T_l	τ	C/F
4.5	1.0	0	0.48	4.65/4
4.5	1.0	.1	.37	3.5/3
4.5	1.0	.3	.16	2/2
4.5	1.0	.6	.07	3.5/3
(b) Transport delay (A)				
ω_n	ζ	A	τ	C/F
15	1.4	0	0.19	2.4/2.25
15	1.4	.105	.29	4.5/3
15	1.4	.24	.43	4.75/3.25
15	1.4	.49	.68	7/7

Figure 1.- Ames Flight Simulator for Advanced Aircraft (FSAA).

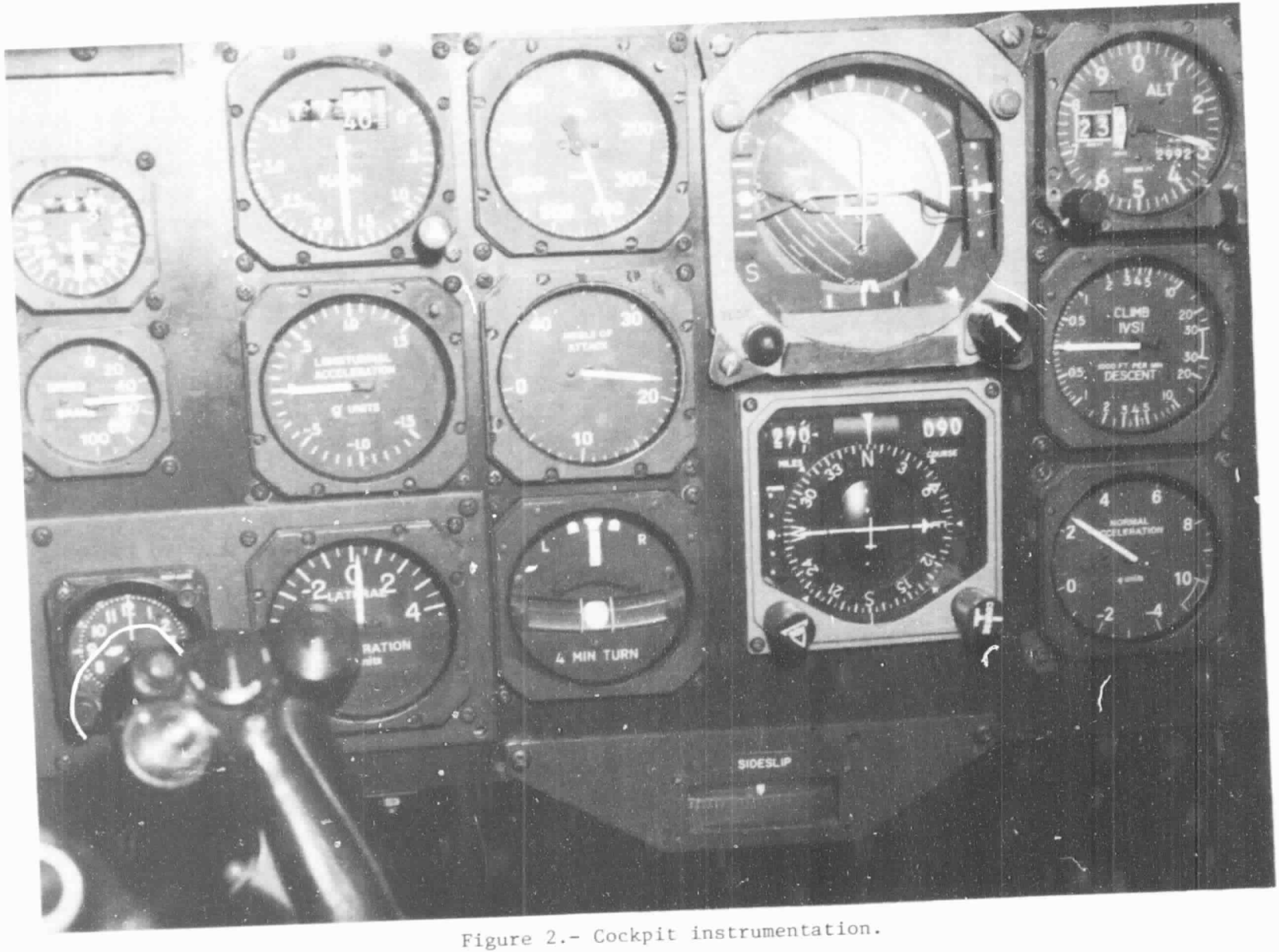

Figure 2.- Cockpit instrumentation.

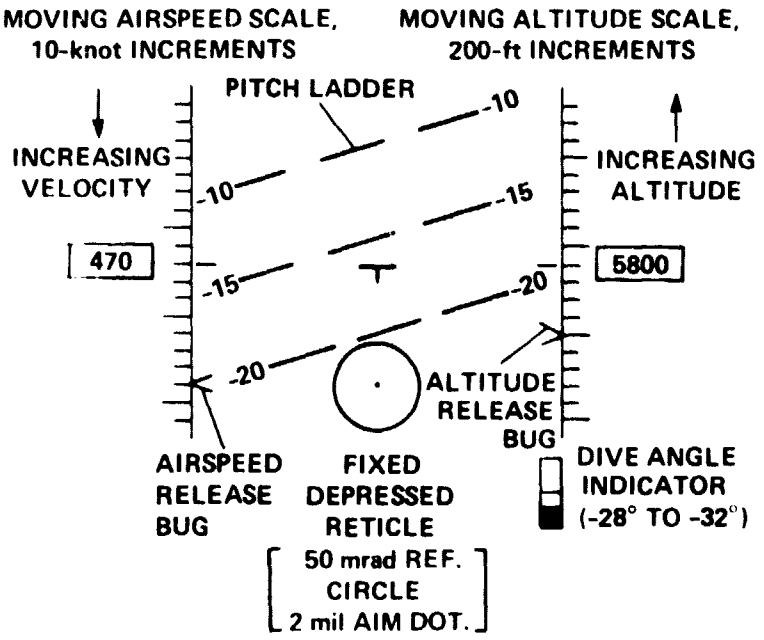

Figure 3.- HUD schematic.

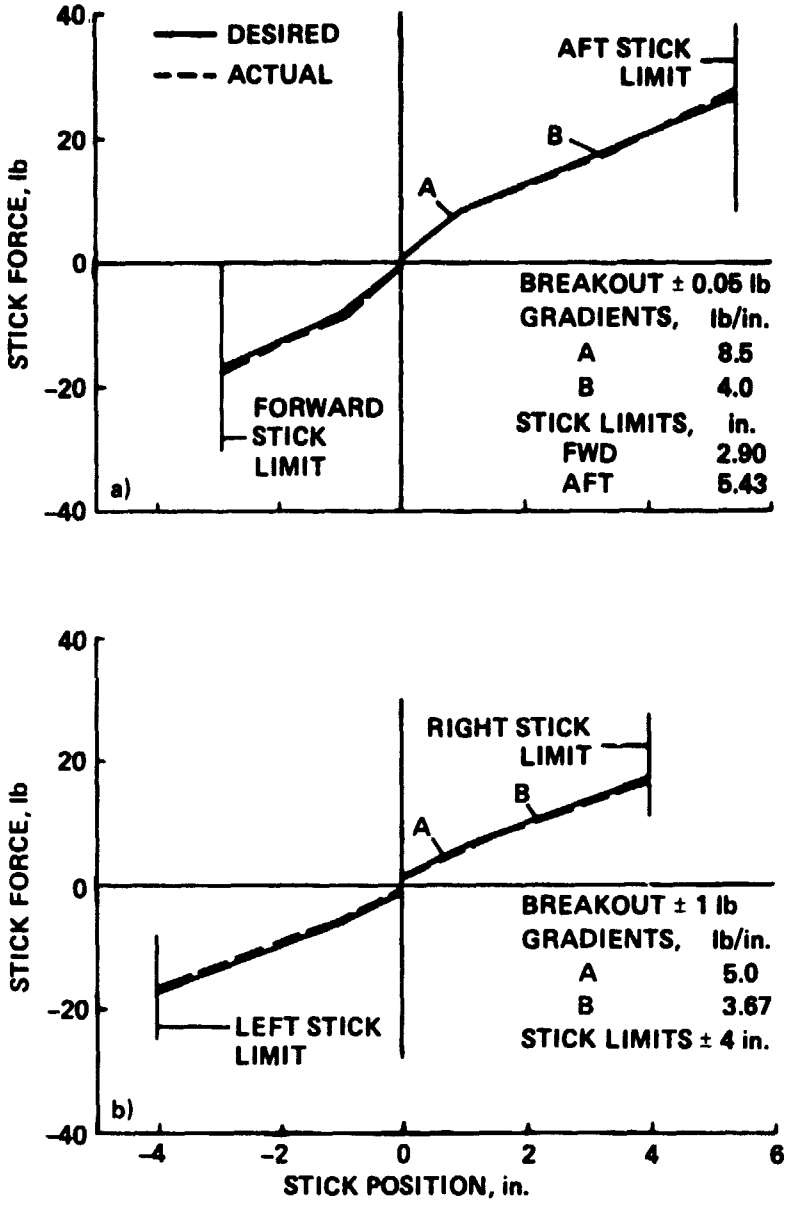

(a) Longitudinal stick.

(b) Lateral stick.

Figure 4.- Force-feel characteristics.

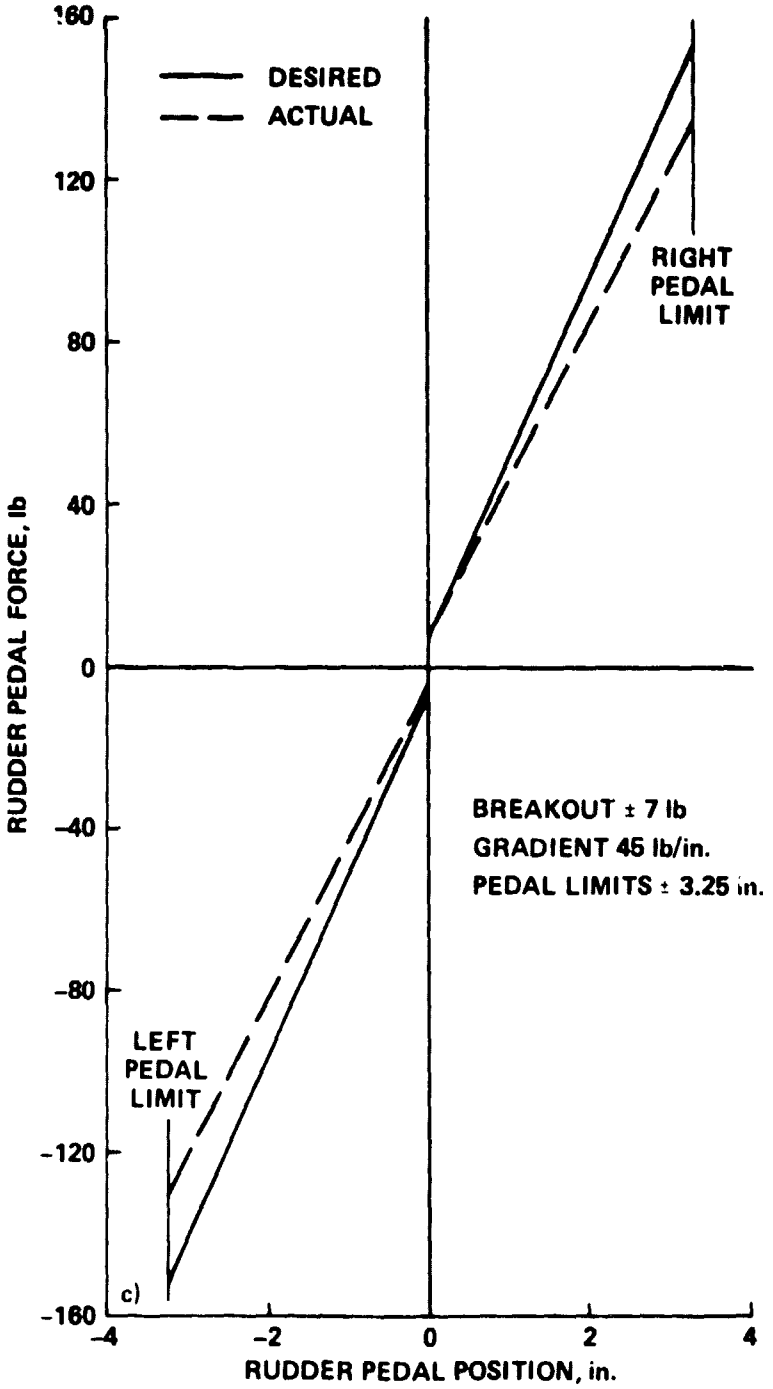

(c) Rudder pedal.

Figure 4.- Concluded.

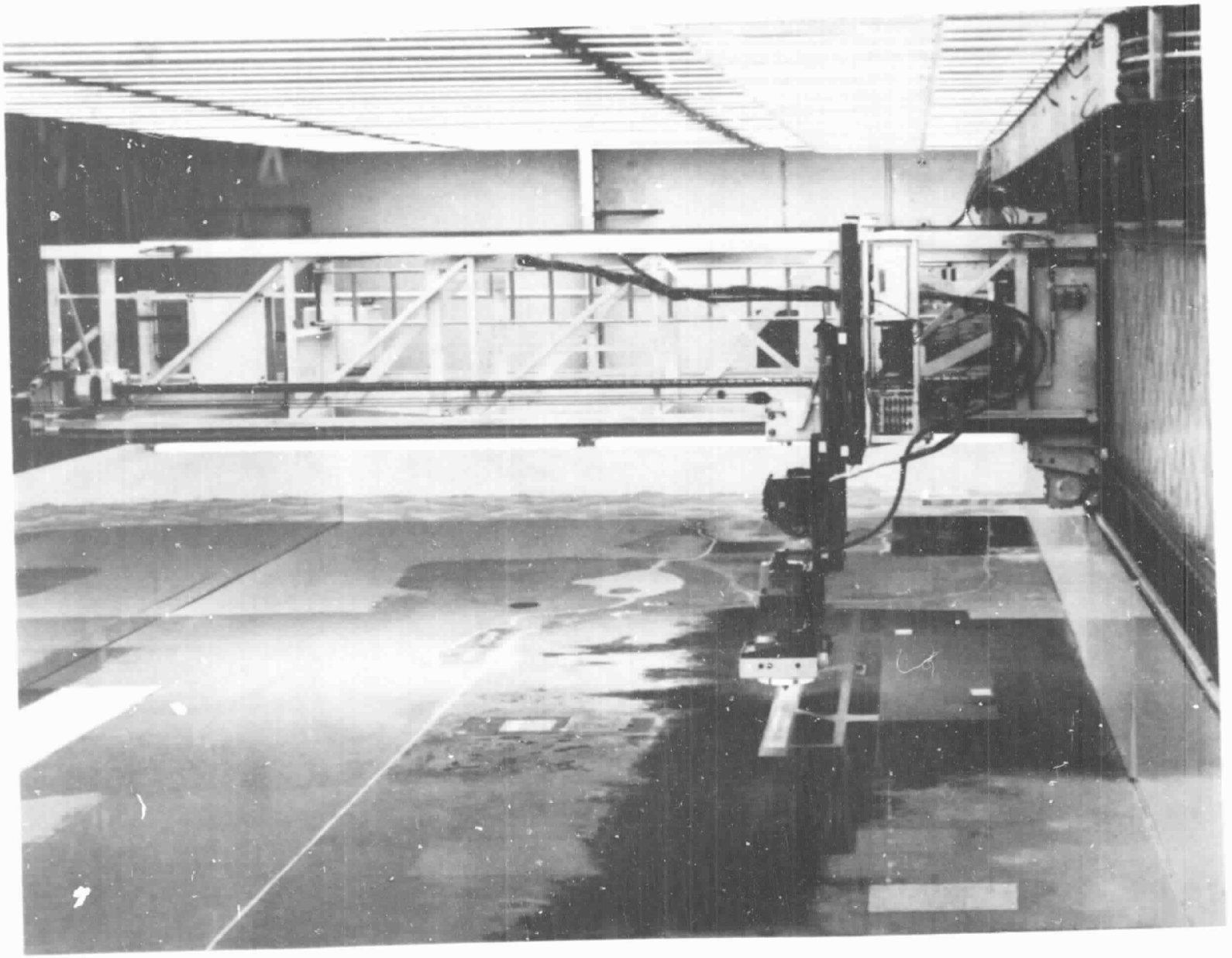

Figure 5.- Terrain board and target location.

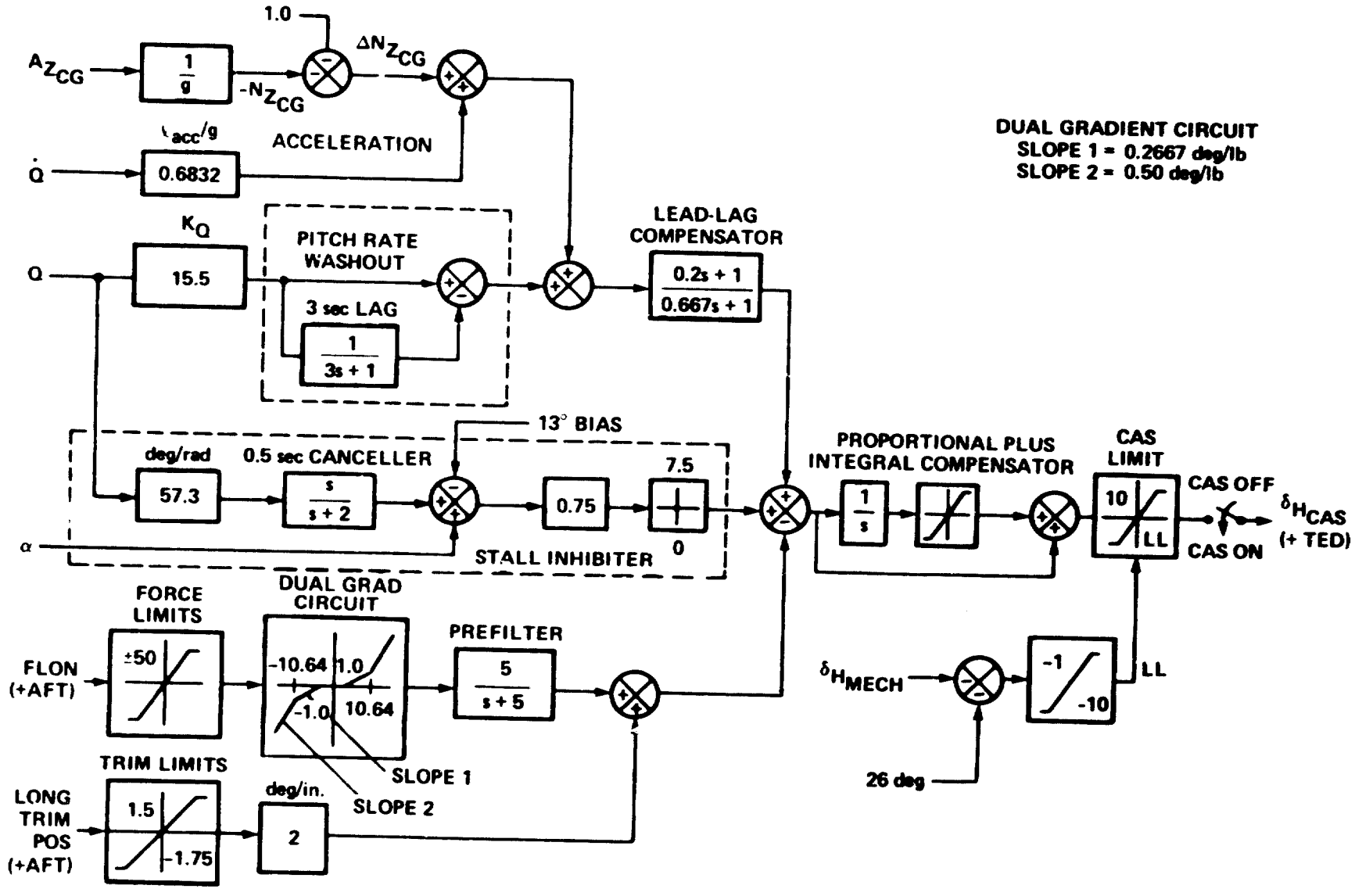

(a) Pitch electrical system (CAS).

Figure 6.- Basic aircraft control systems.

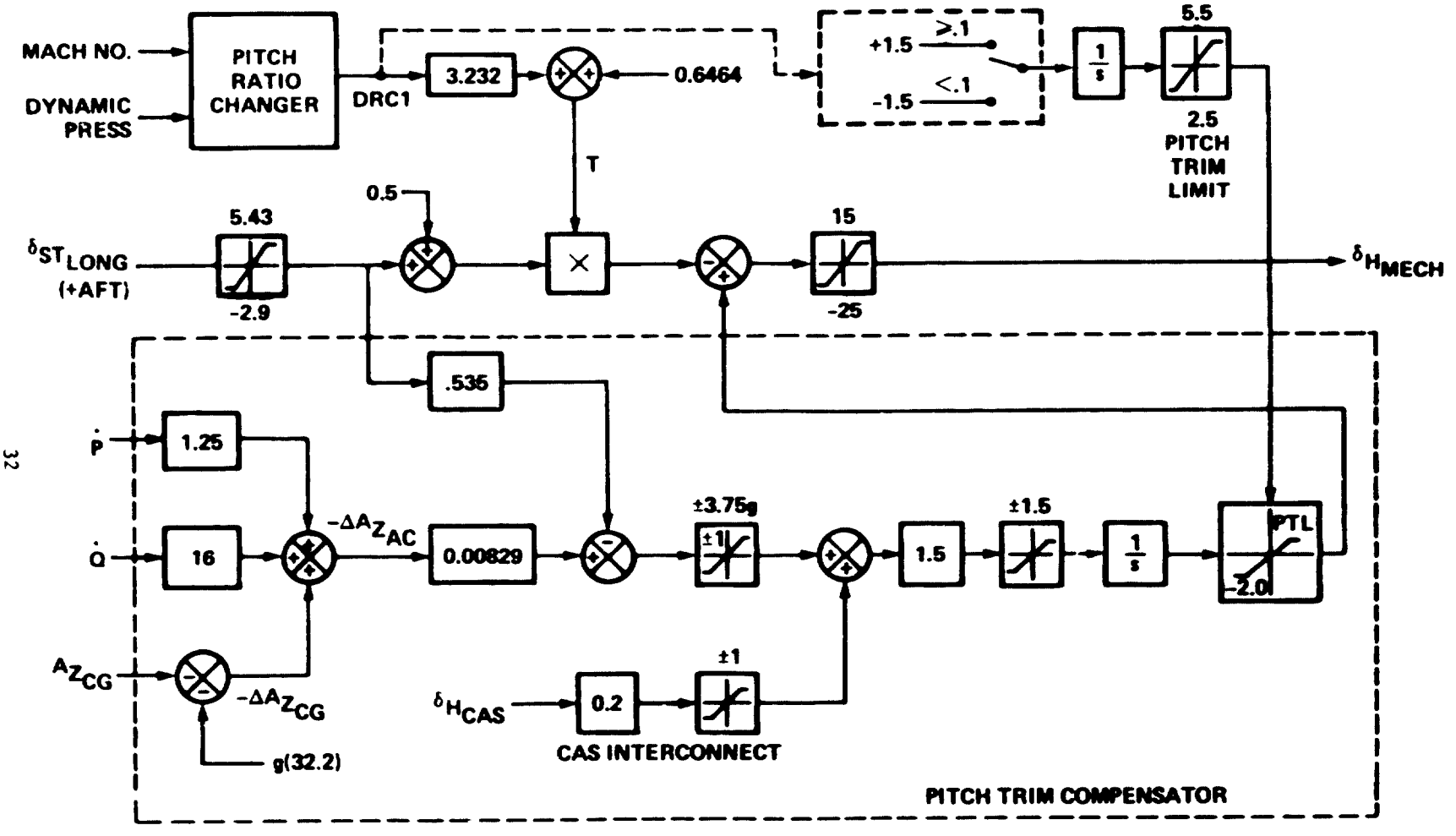

(b) Pitch mechanical system.

Figure 6.- Continued.

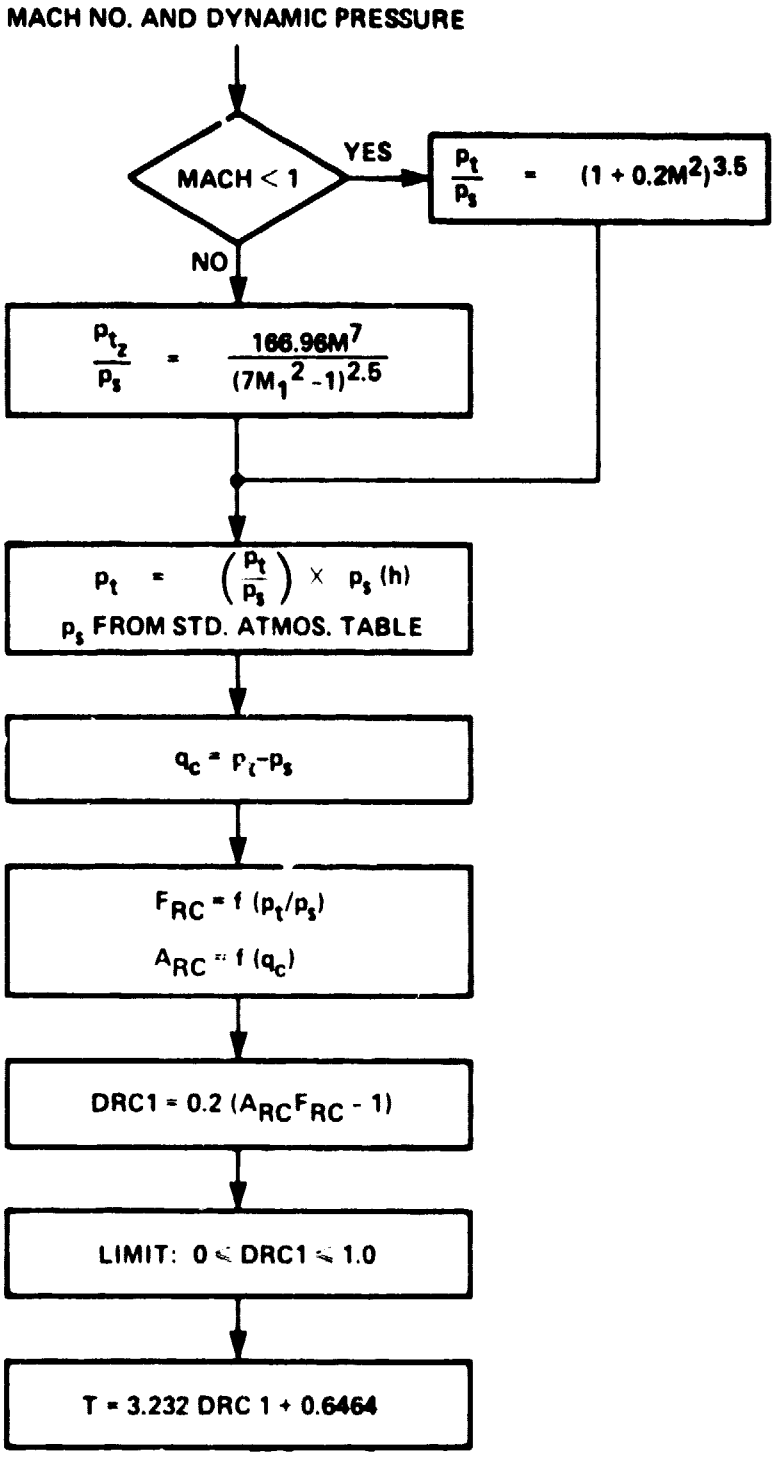

(c) Pitch ratio changer mechanization.

Figure 6.- Continued.

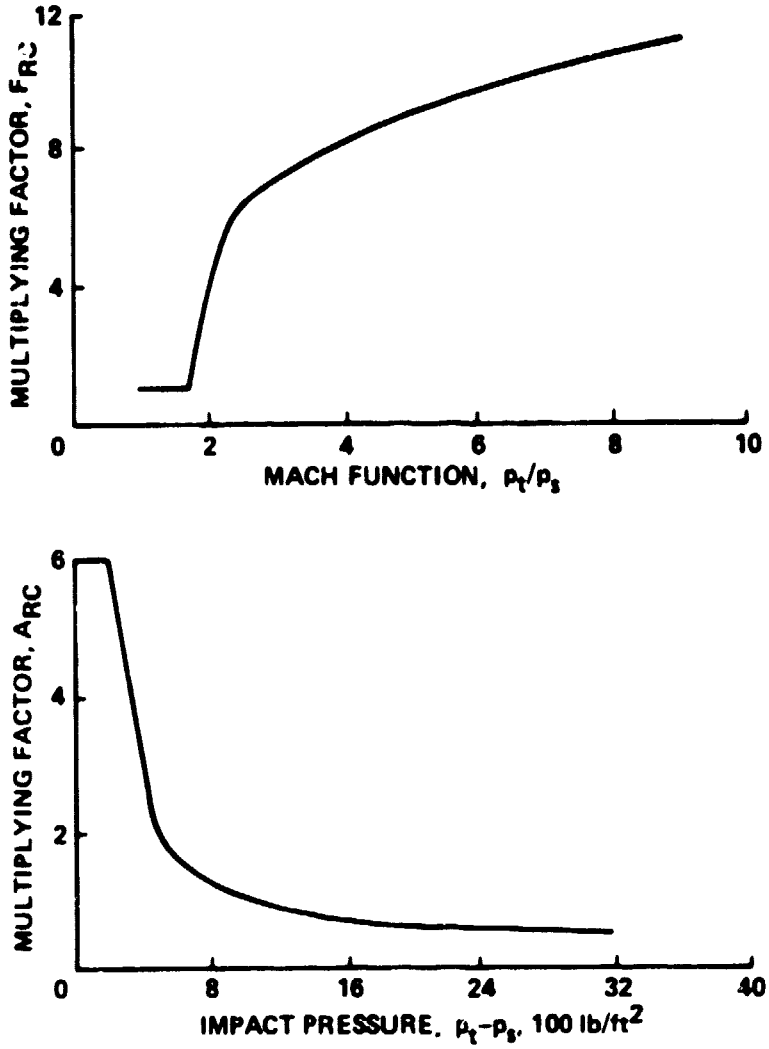

(d) Pitch ratio changer multiplying factors.

Figure 6.- Continued.

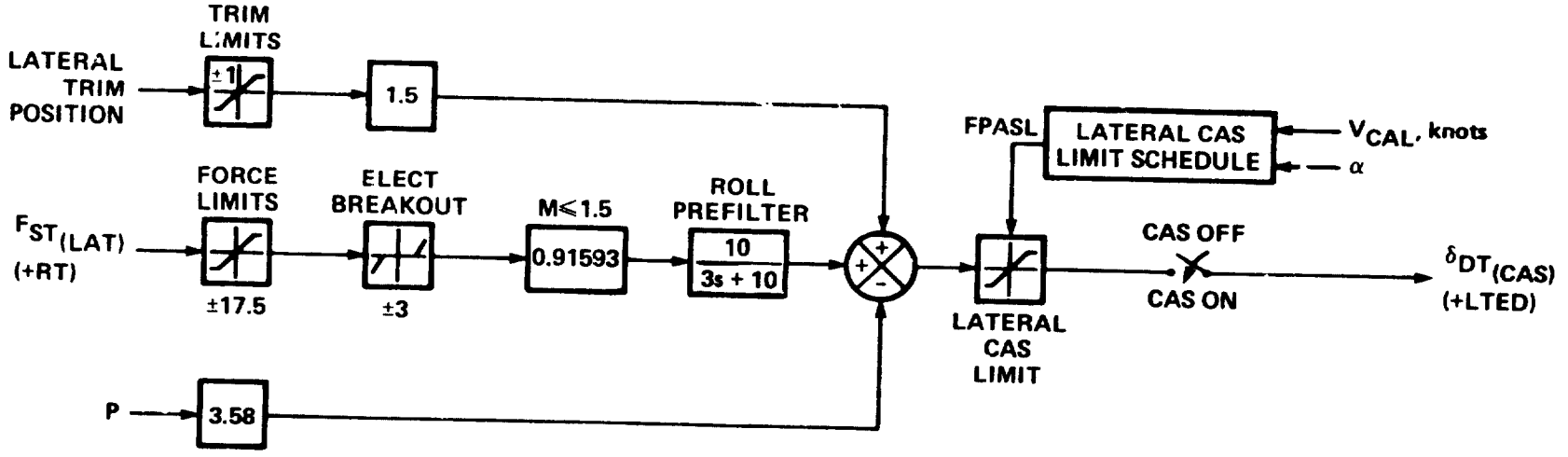

(e) Roll electrical system (CAS).

Figure 6.- Continued.

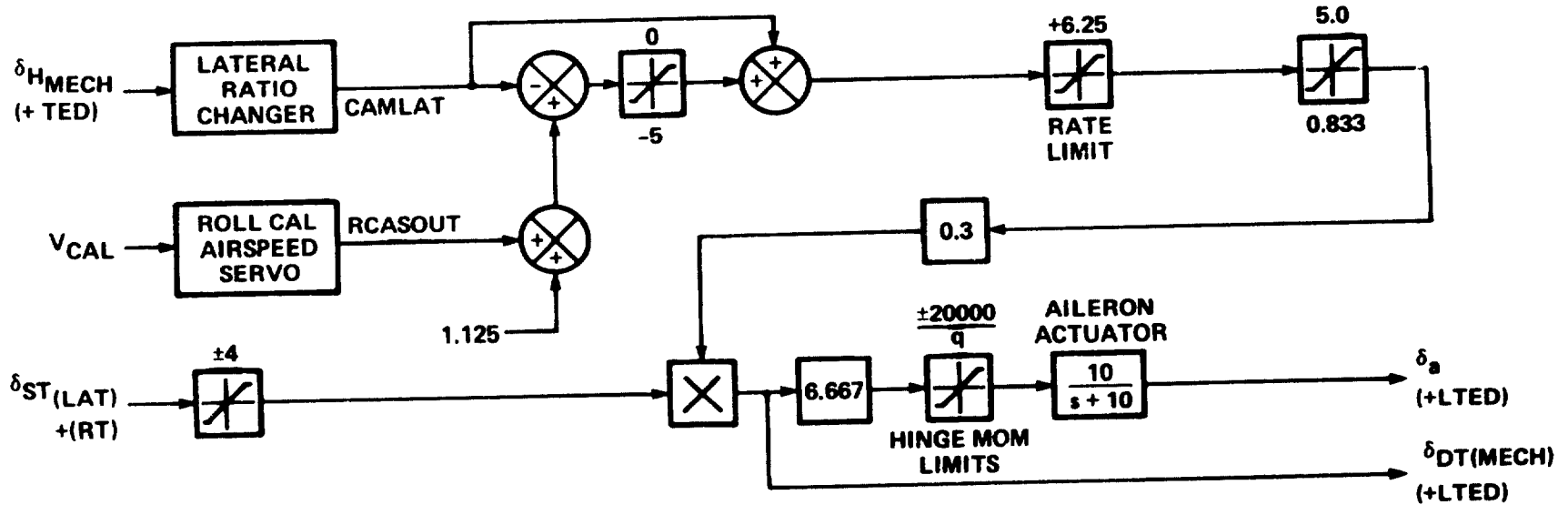

(f) Roll mechanical system.

Figure 6.- Continued.

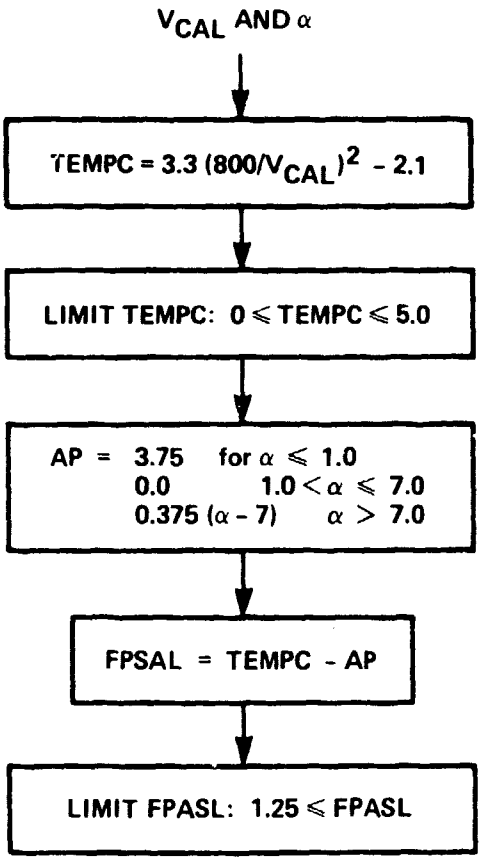

(g) Lateral CAS limit schedule.

Figure 6.- Continued.

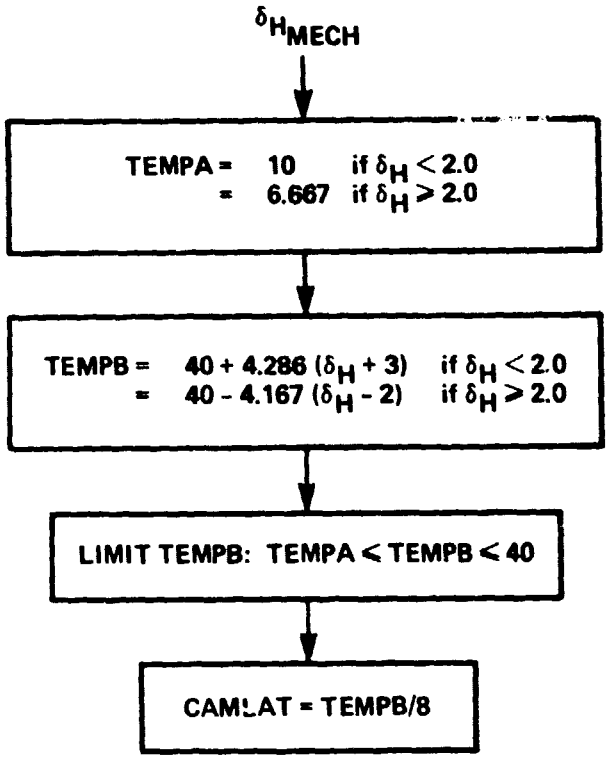

(h) Lateral ratio changer.

Figure 6.- Continued.

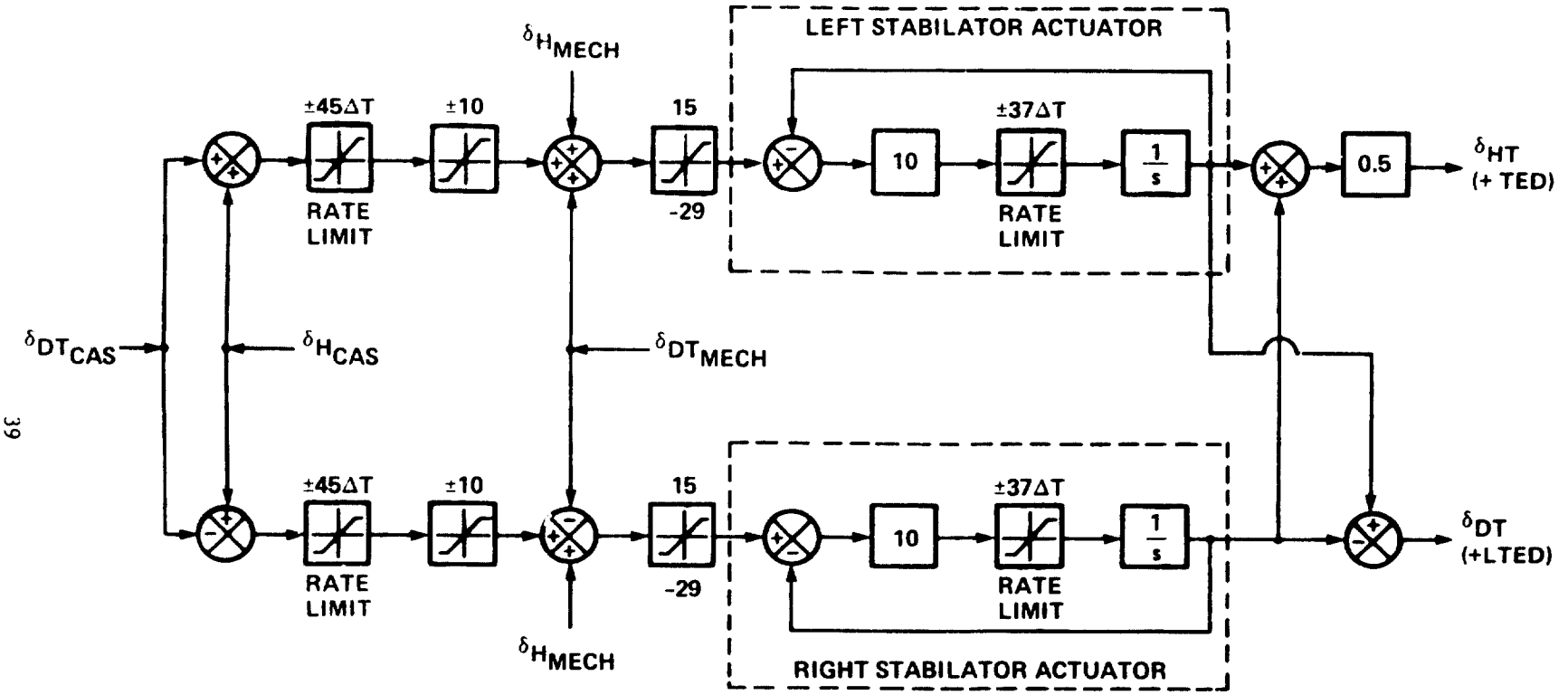

(i) Pitch/roll mixing linkage, series servos and stabilator power actuators.

Figure 6.- Continued.

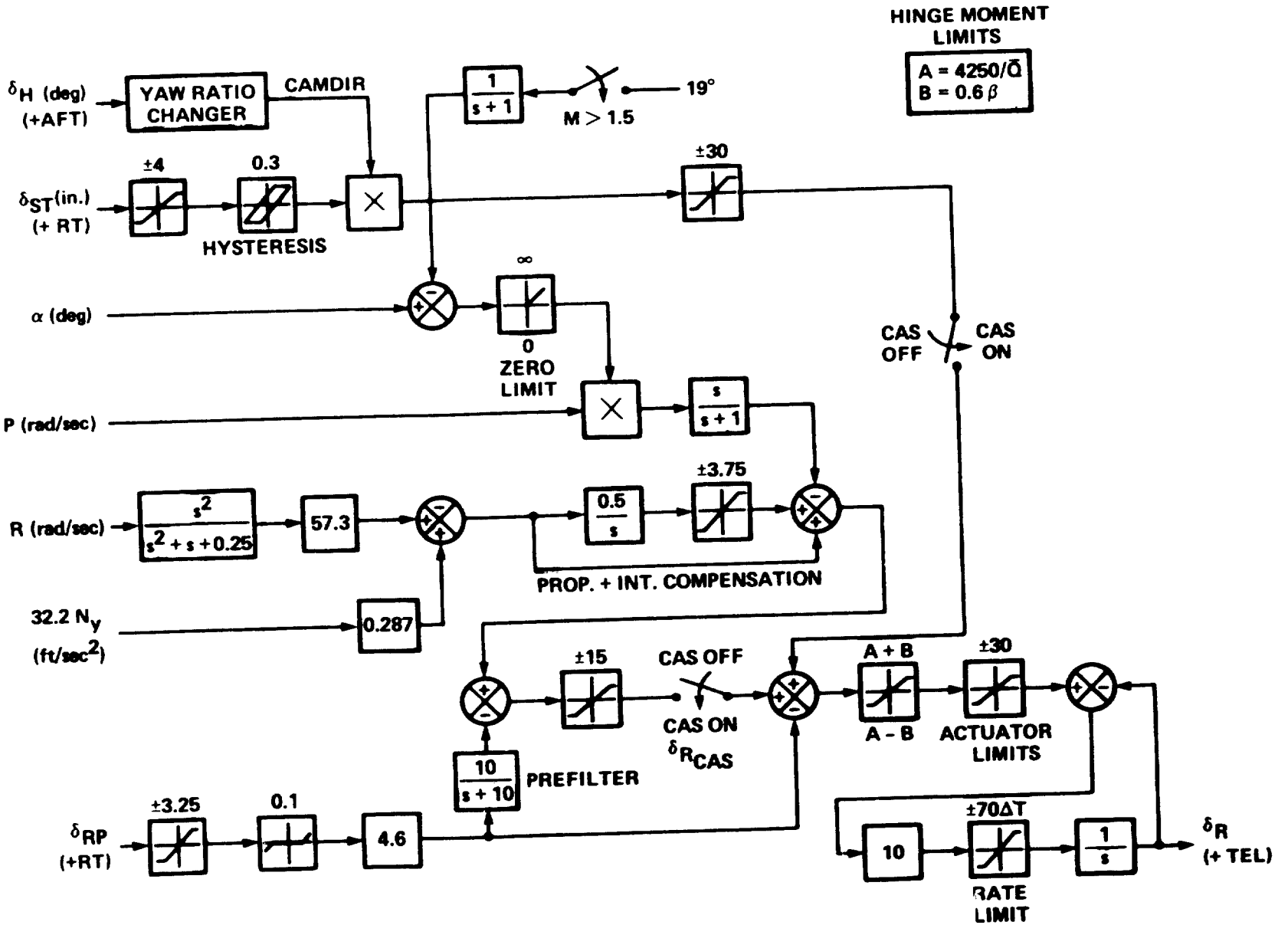

(j) Yaw control system.

Figure 6.- Continued.

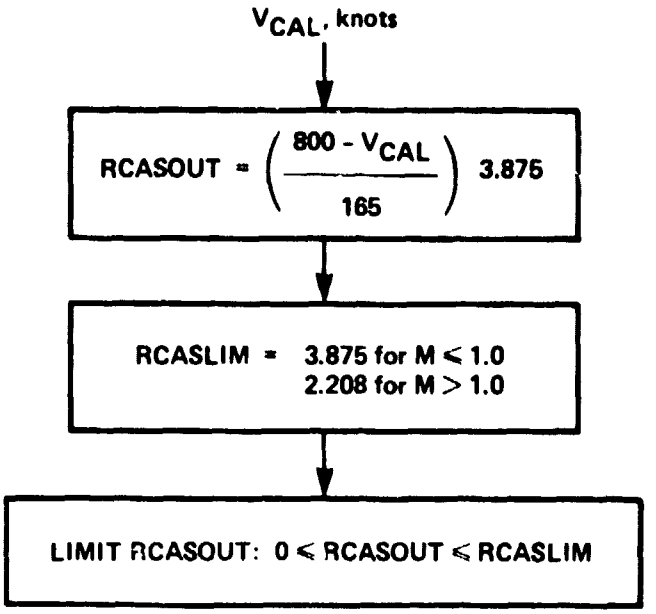

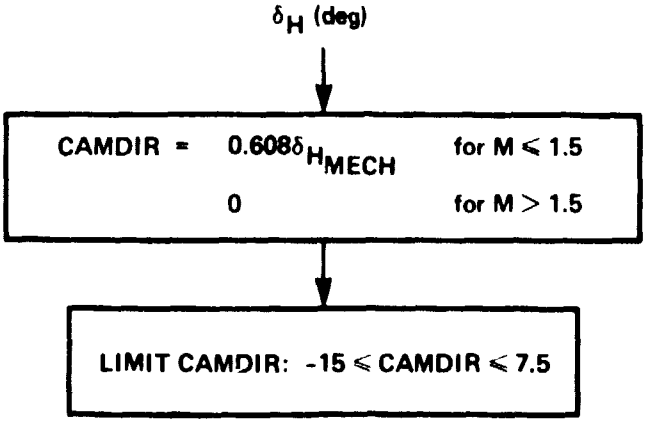

(k) Yaw ratio changer.

Figure 6.- Concluded.

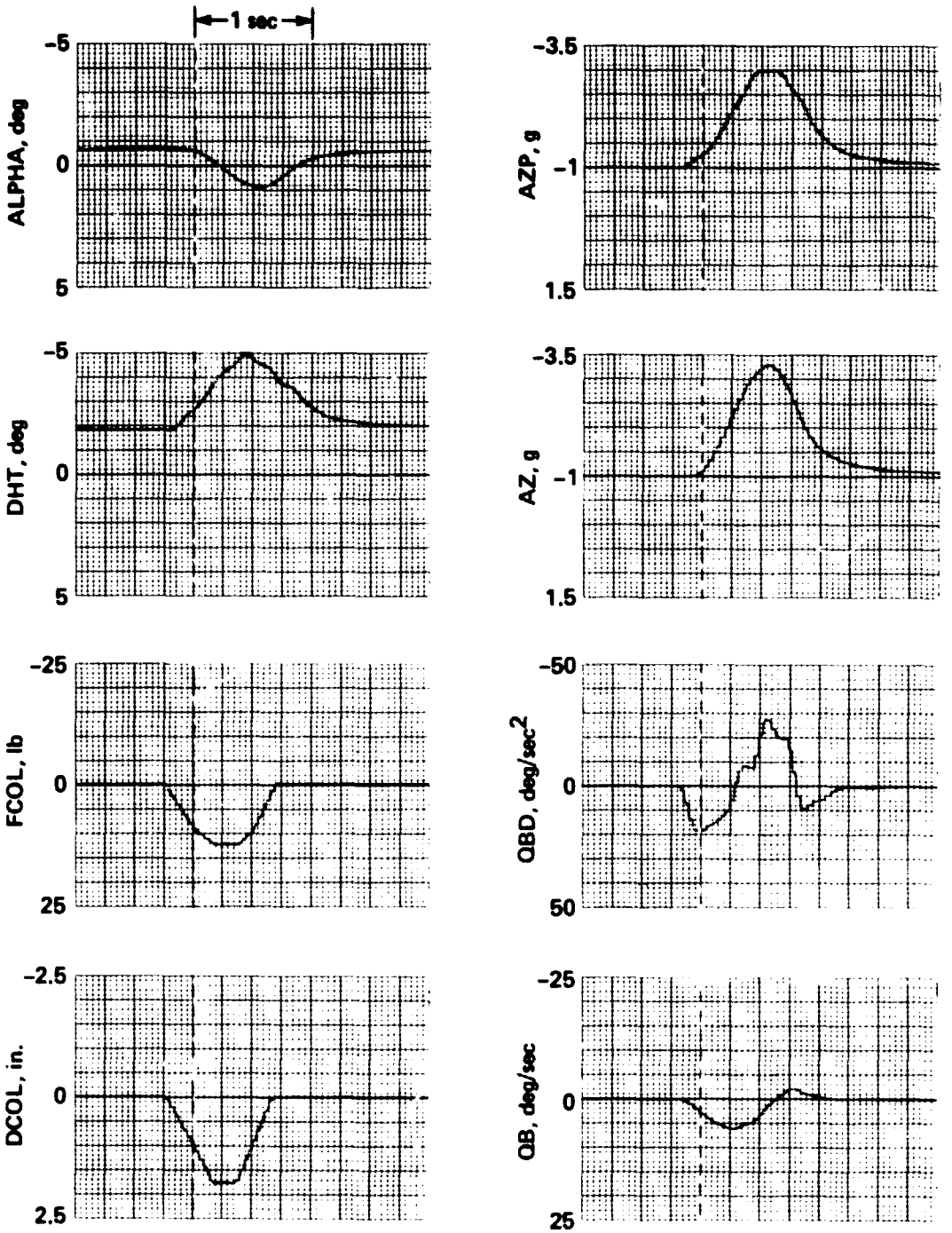

Figure 7.- Aircraft response to longitudinal step input.

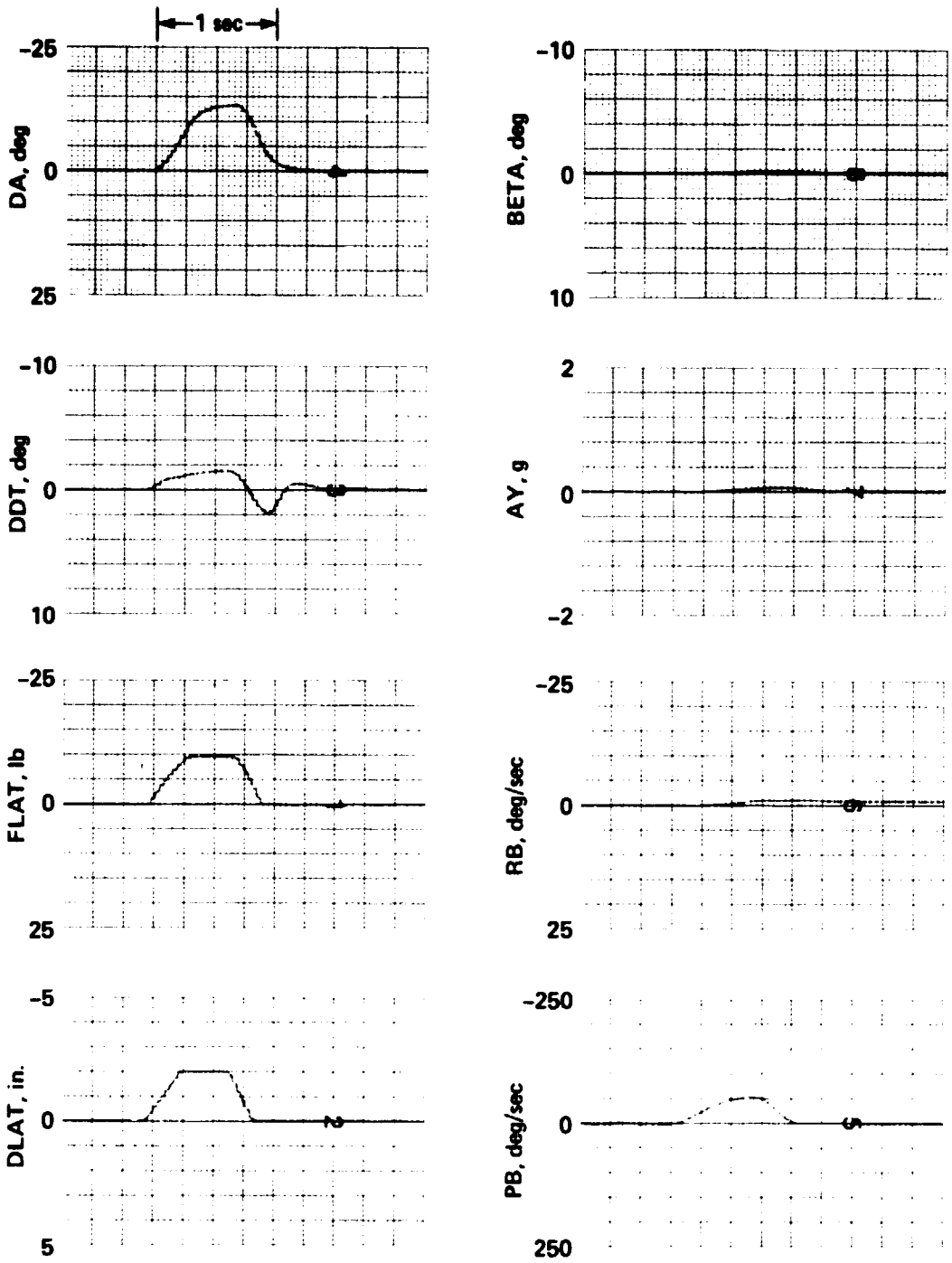

Figure 8.- Aircraft response to lateral step input.

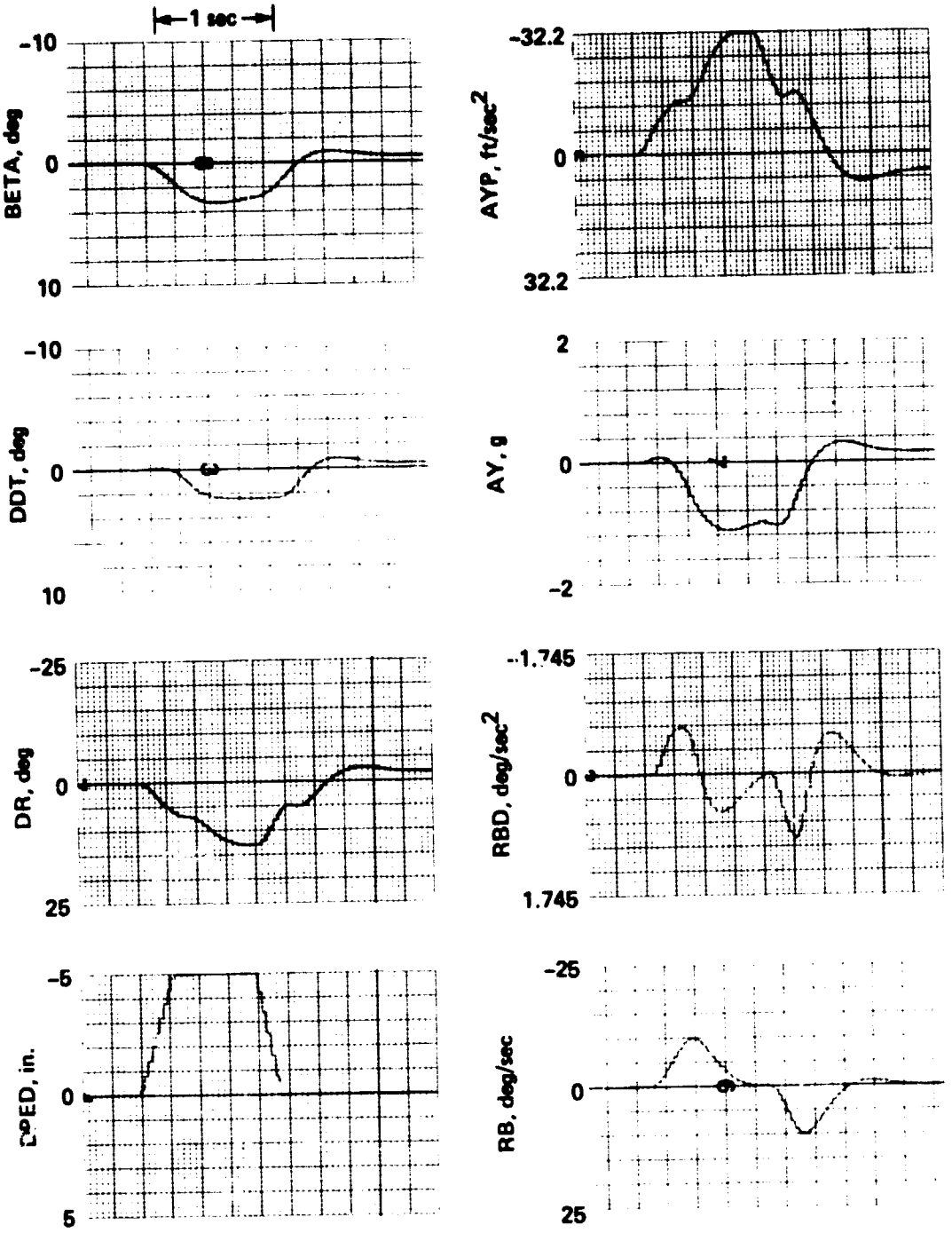

Figure 9.- Aircraft response to pedal step input.

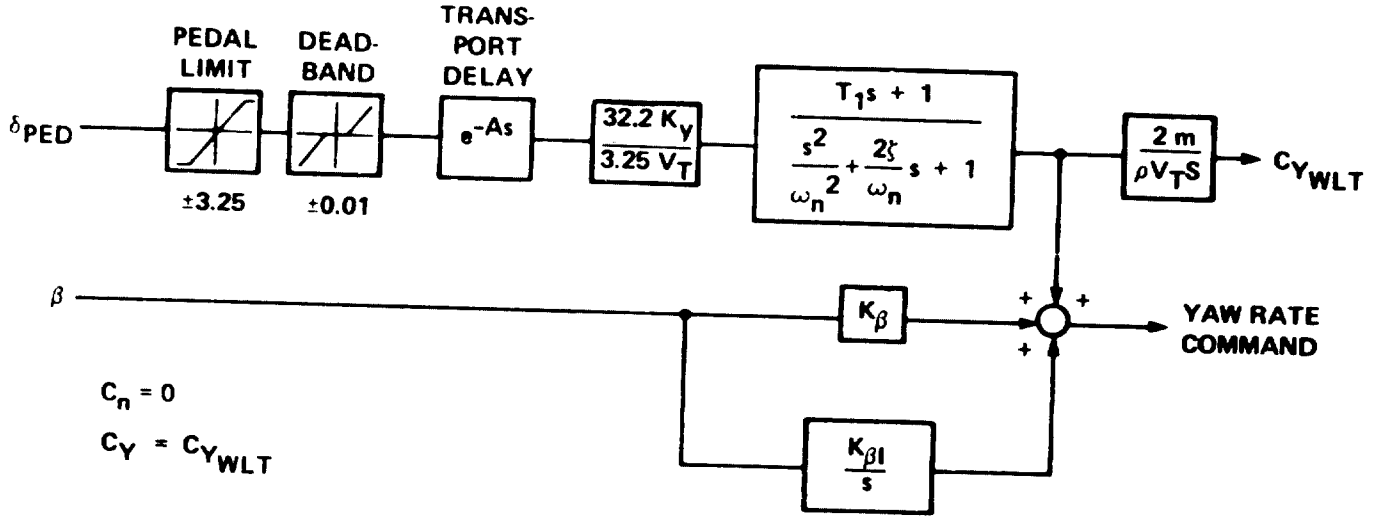

Figure 10.- Wings-level-turn mechanization.

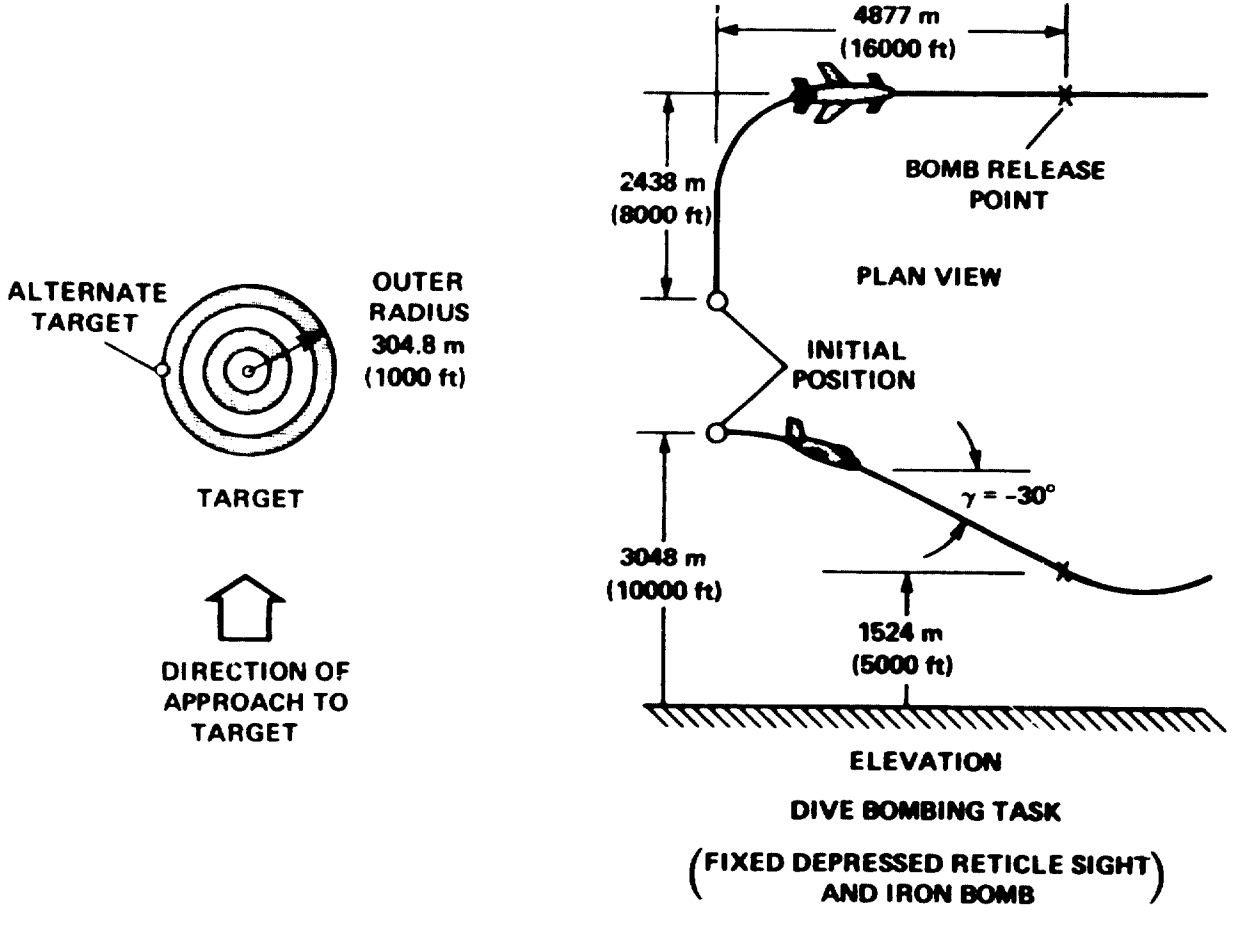

Figure 11.- Dive-bombing task and bull's-eye target.

PILOT COMMENT CARD

1. **INITIAL IMPRESSIONS OF CONFIGURATION**
2. **AIRCRAFT RESPONSE TO CONTROL INPUTS**
   (RESPONSE TIME, OVERSHOOT, DAMPING, SETTLING TIME, ETC.)
3. **CONTROL FORCES AND SENSITIVITY**
   (FORCES, DISPLACEMENTS AND HARMONY)
4. **MISSION PERFORMANCE**
   (ABILITY TO ACQUIRE TARGET AND TO MAKE EITHER LARGE OR SMALL POSITION CORRECTIONS)
5. **COOPER-HARPER RATING**
   - **OVERALL TASK**
   - **PARAMETER BEING EVALUATED**
6. **SUMMARY COMMENTS**
   (REASONS FOR C-H RATINGS AND ANY SPECIAL COMMENTS PERTAINING TO THE EVALUATION)

HANDLING QUALITIES RATING SCALE

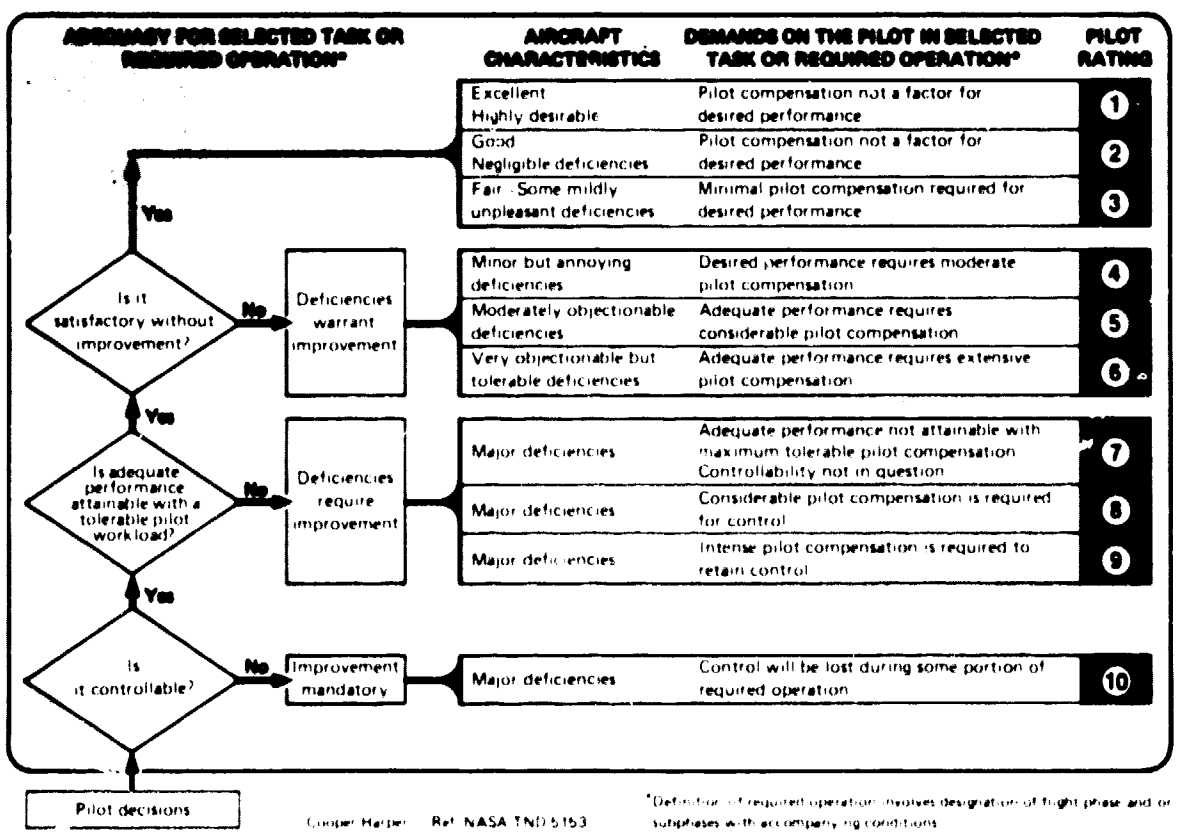

Figure 12.- Pilot comment card and rating scale.

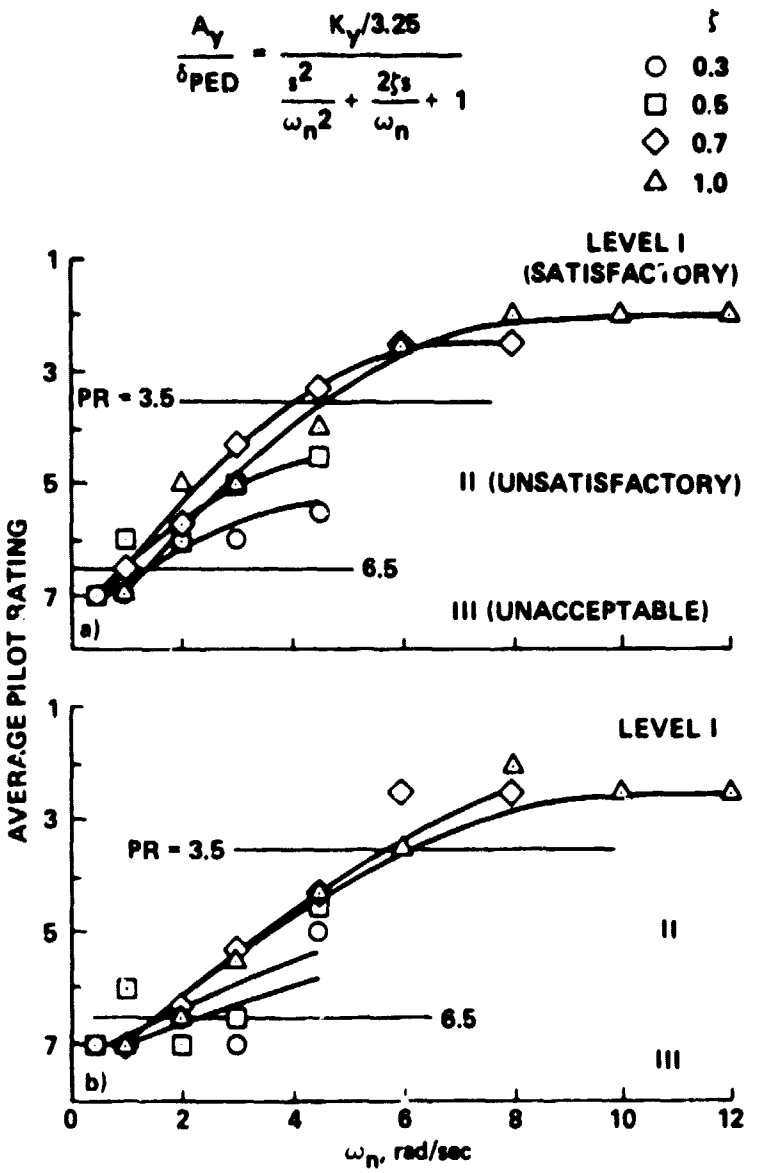

(a) Fine task.

(b) Coarse task.

Figure 13.- Effect of natural frequency on pilot rating, Pilot A.

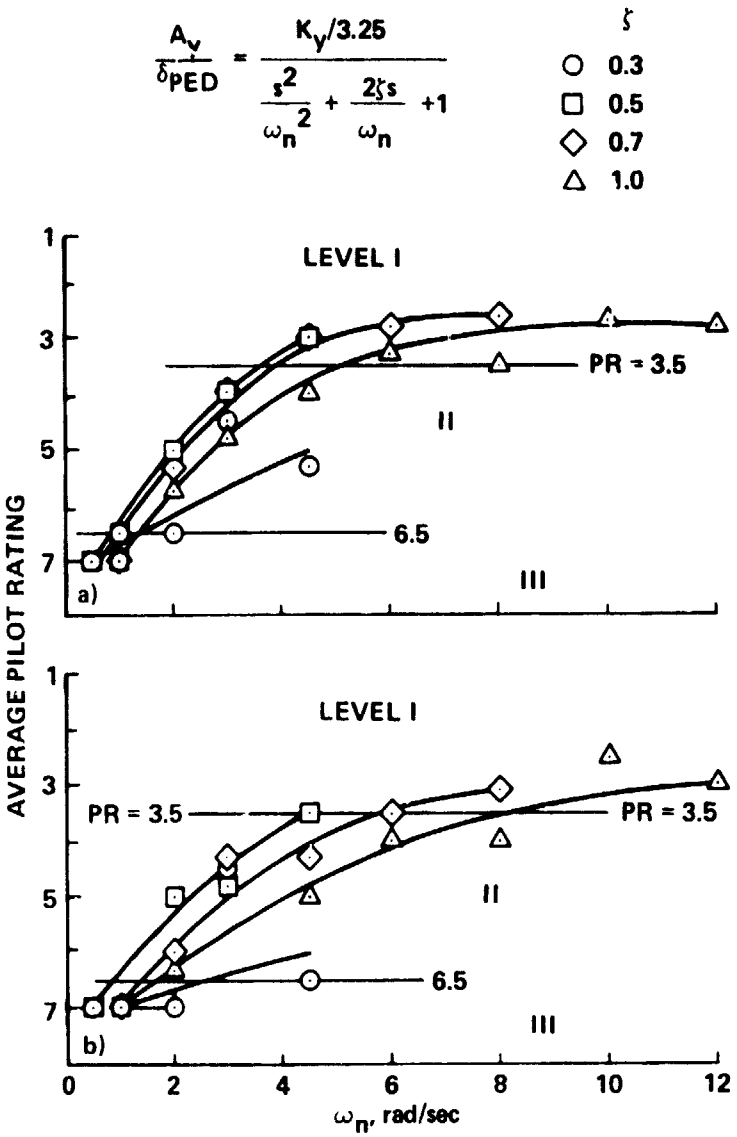

(a) Fine task.

(b) Coarse task.

Figure 14.- Effect of natural frequency on pilot rating, Pilot B.

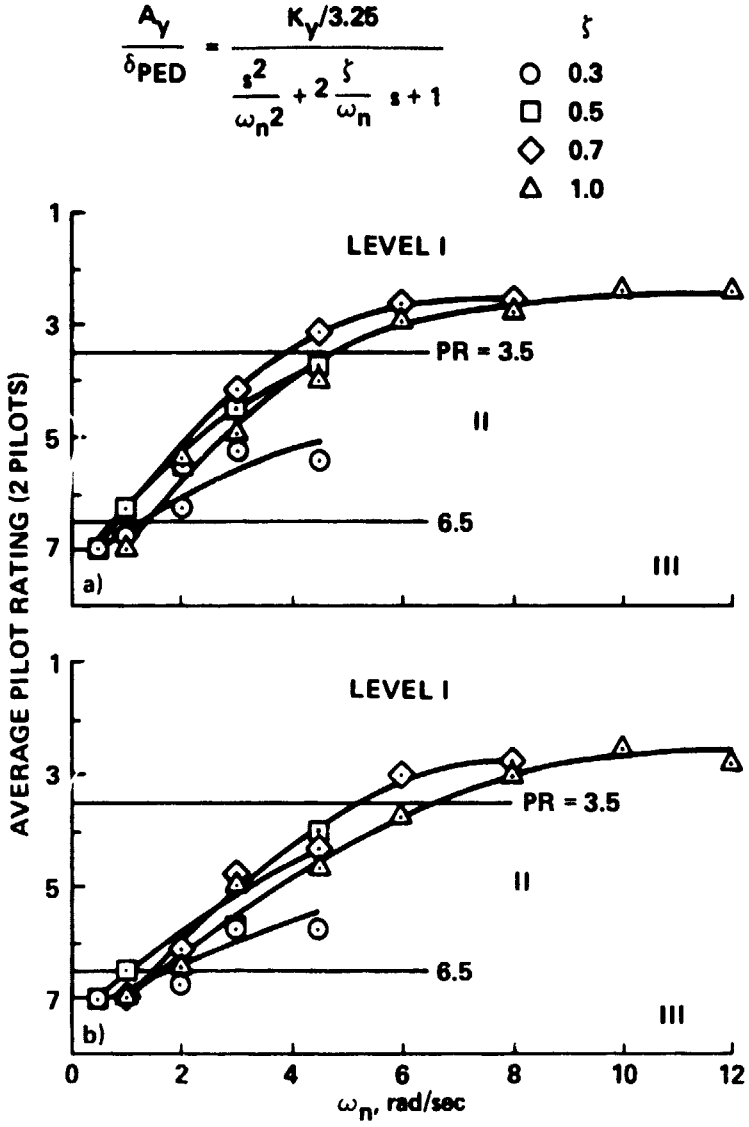

(a) Fine task.

(b) Coarse task.

Figure 15.- Effect of natural frequency on pilot rating, Pilots A and B.

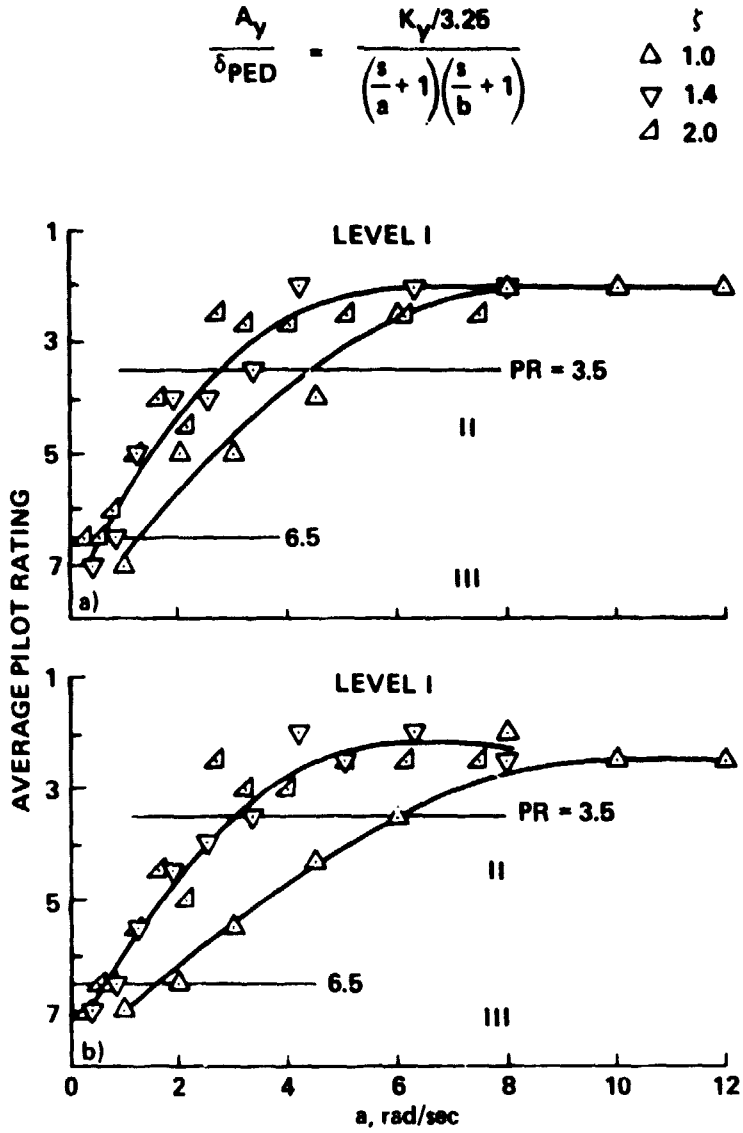

(a) Fine task.

(b) Coarse task.

Figure 16.- Effect of low-frequency root on pilot rating, Pilot A.

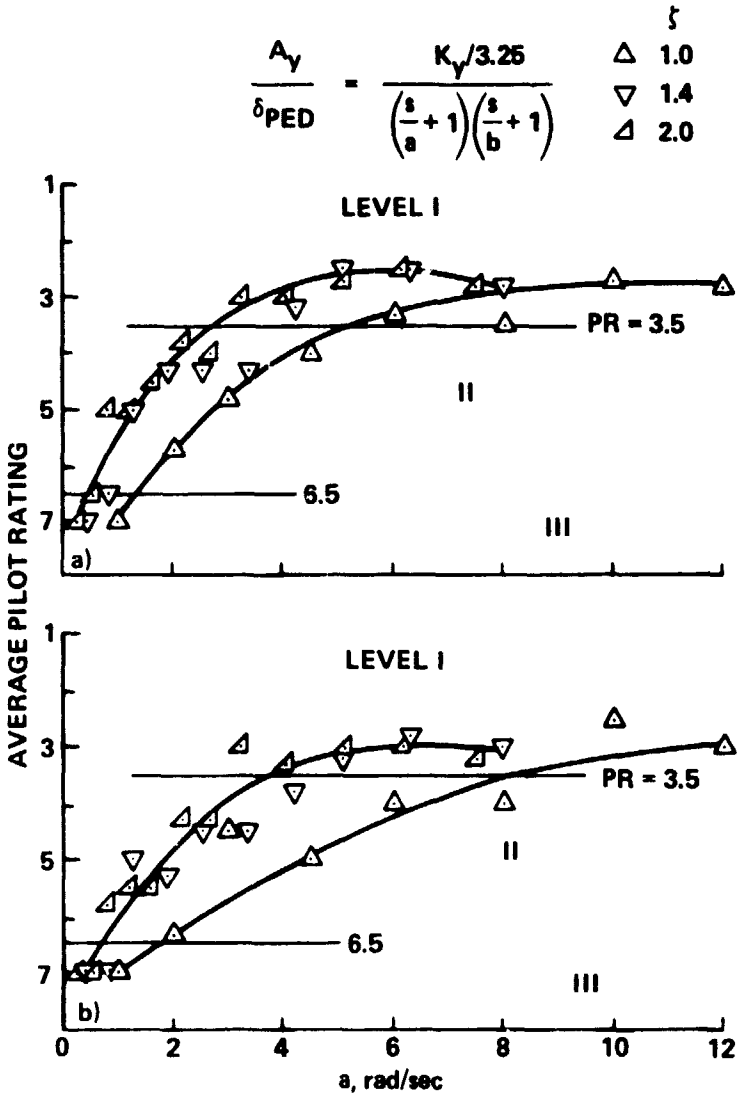

(a) Fine task.

(b) Coarse task.

Figure 17.- Effect of low-frequency root on pilot rating, Pilot B.

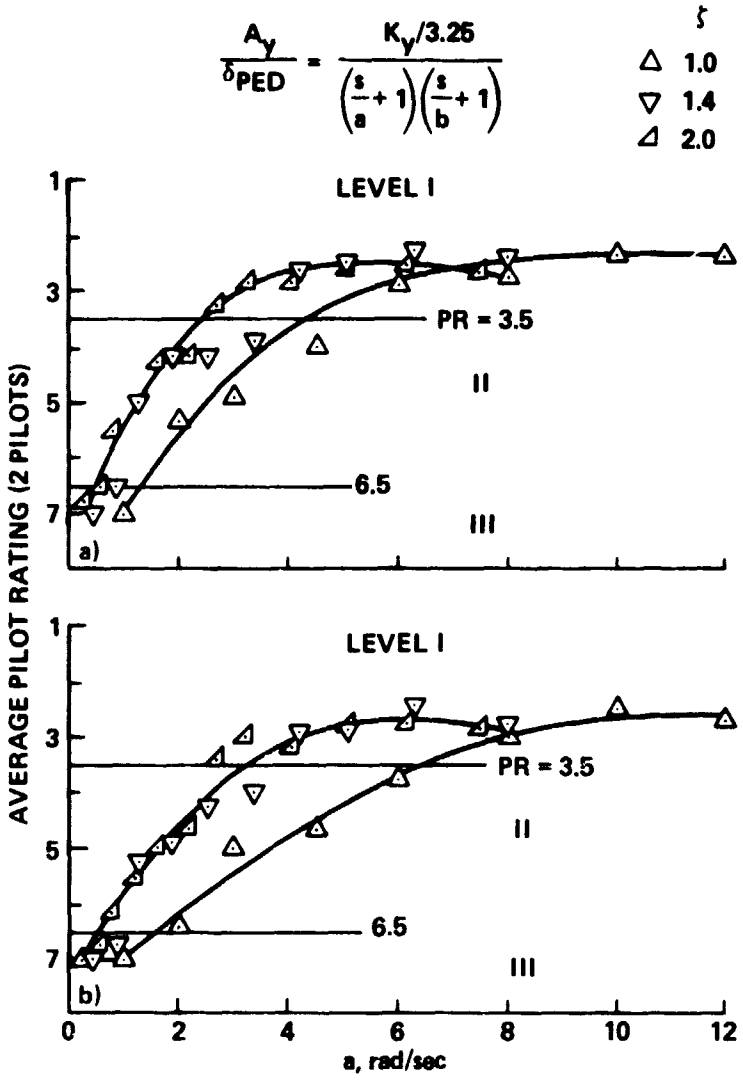

(a) Fine task.

(b) Coarse task.

Figure 18.- Effect of low-frequency root on pilot rating, Pilots A and B.

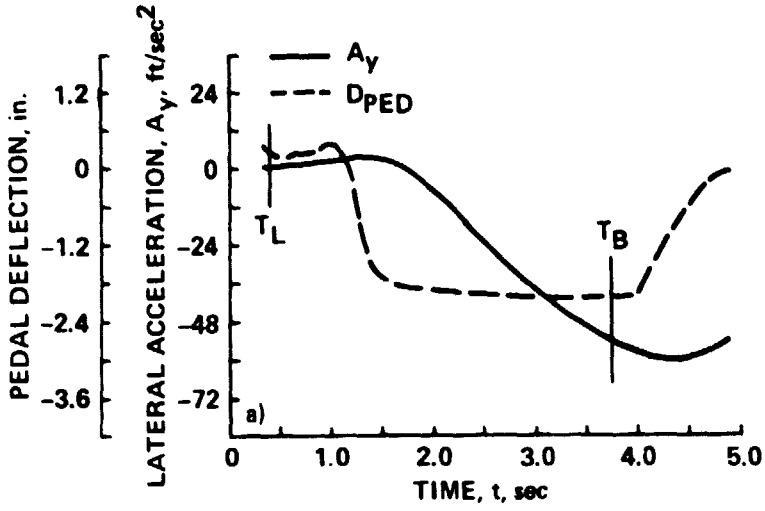

(a) ω_n = 1.0.

Figure 19.- Effect of frequency on the time history of the lateral acceleration response to pedal input, ζ = 0.7.

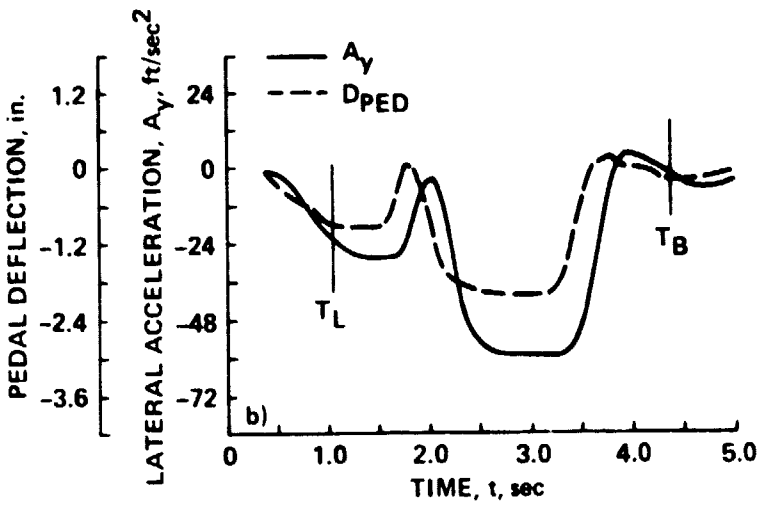

(b) $\omega_n = 8.0$.

Figure 19.- Concluded.

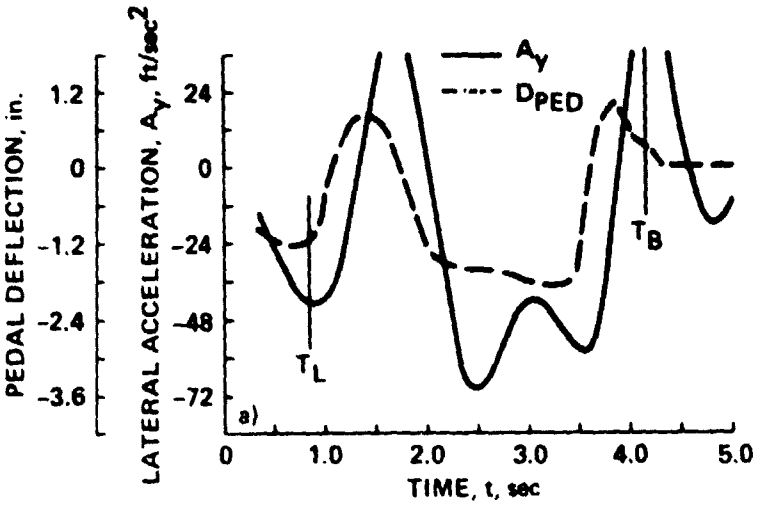

(a) $\zeta = 0.3$.

Figure 20.- Effect of damping ratio on the time history of the lateral acceleration response to pedal input; $\omega_n = 4.5$, $\zeta < 1.0$.

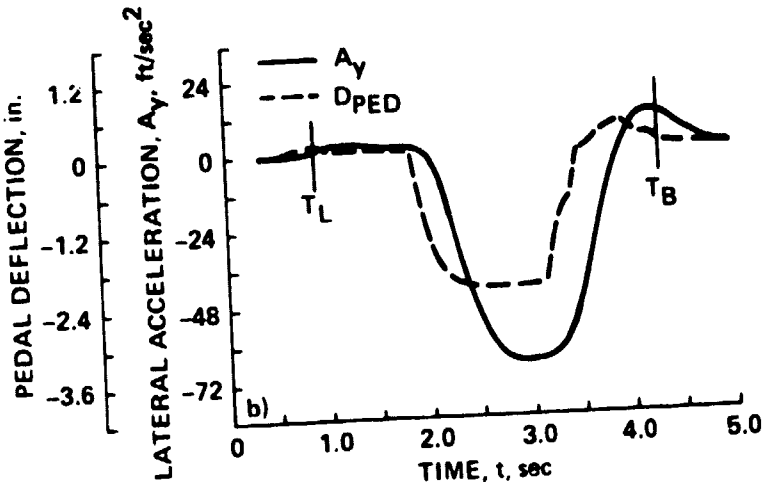

(b) $\zeta = 0.7$.

Figure 20.- Concluded.

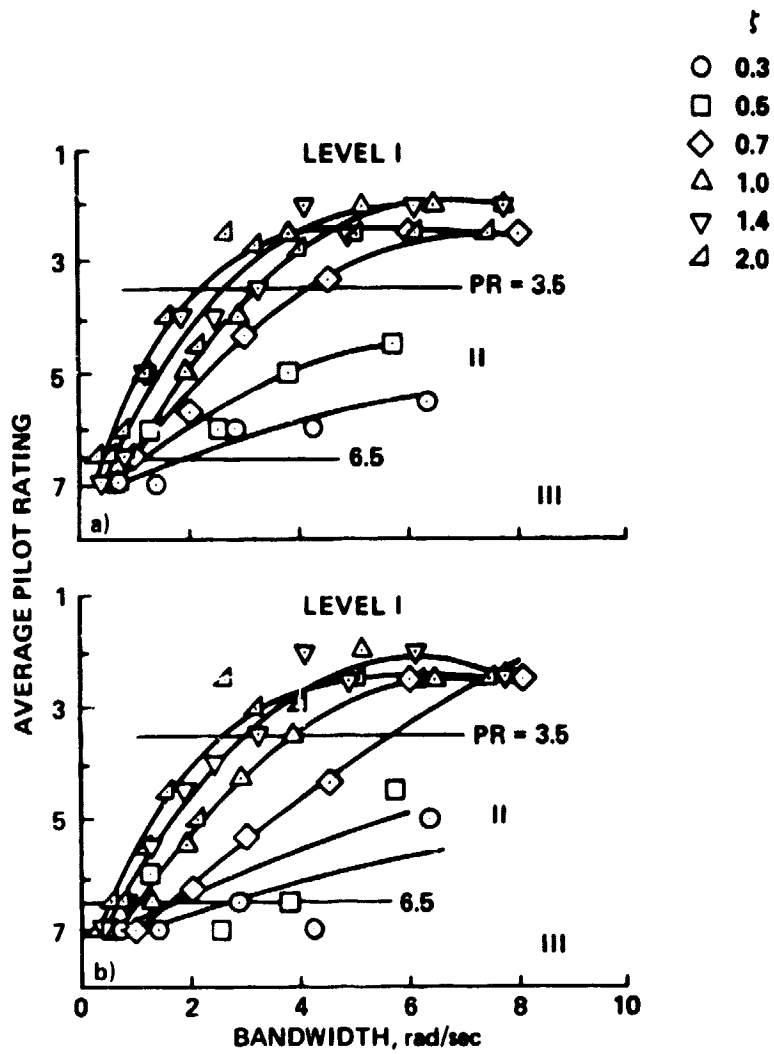

(a) Fine task.

(b) Coarse task.

Figure 21.- Effect of bandwidth on pilot rating, Pilot A.

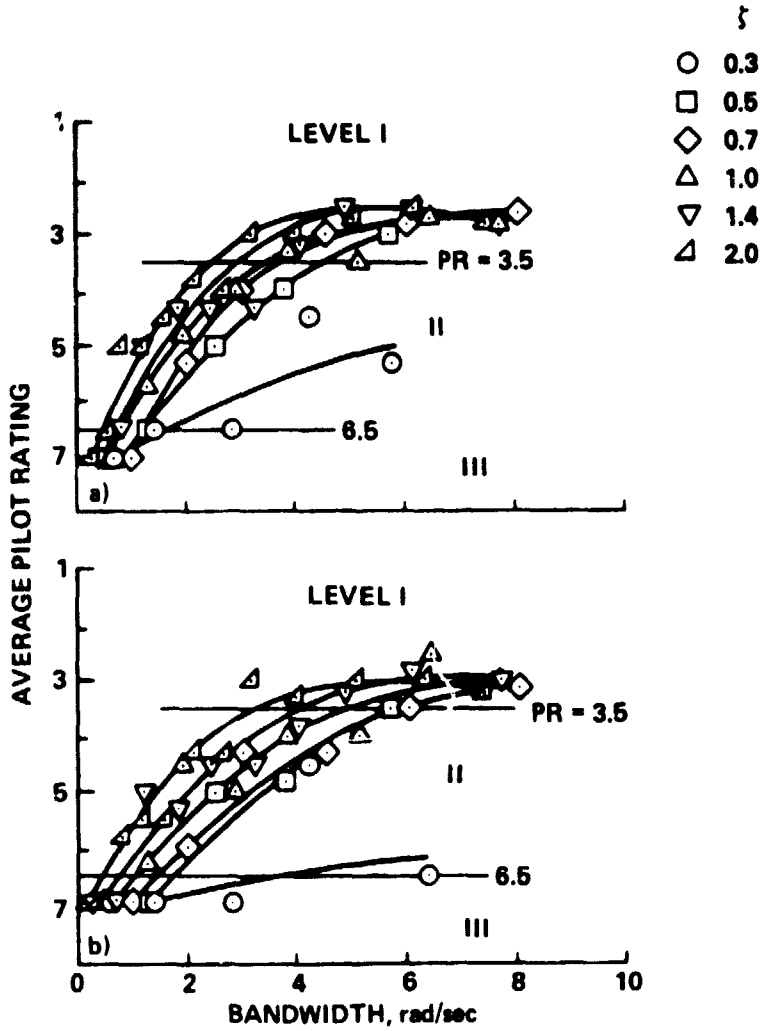

(a) Fine task.

(b) Coarse task.

Figure 22.- Effect of bandwidth on pilot rating, Pilot B.

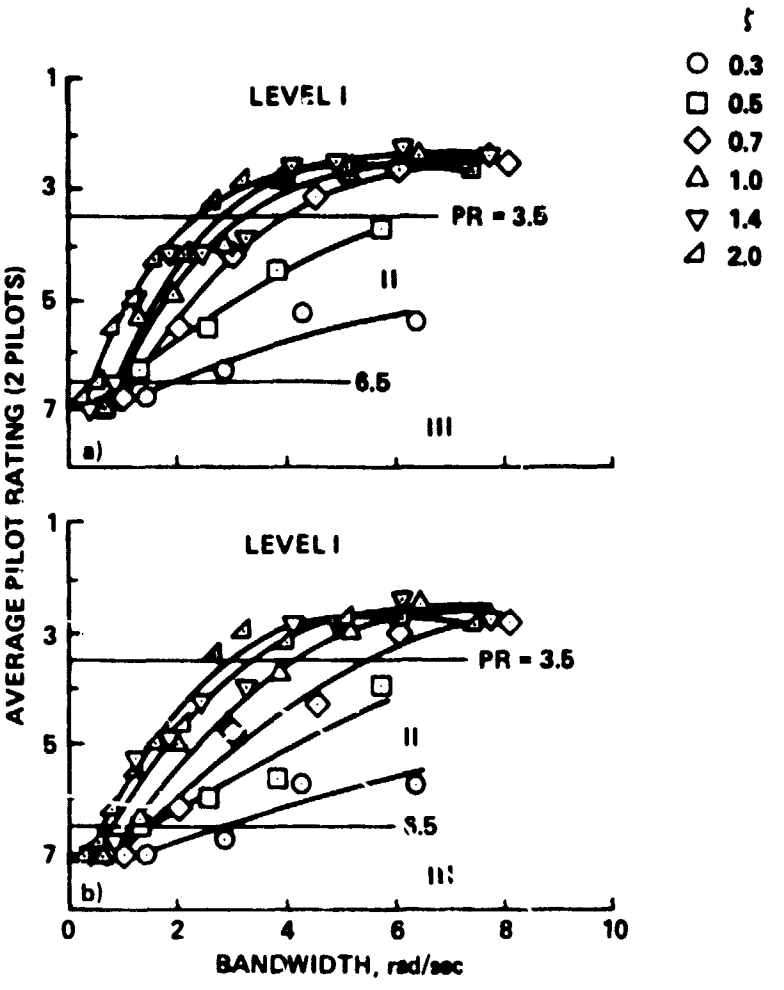

(a) Fine task.

(b) Coarse task.

Figure 23.- Effect of bandwidth on pilot rating, Pilots A and B.

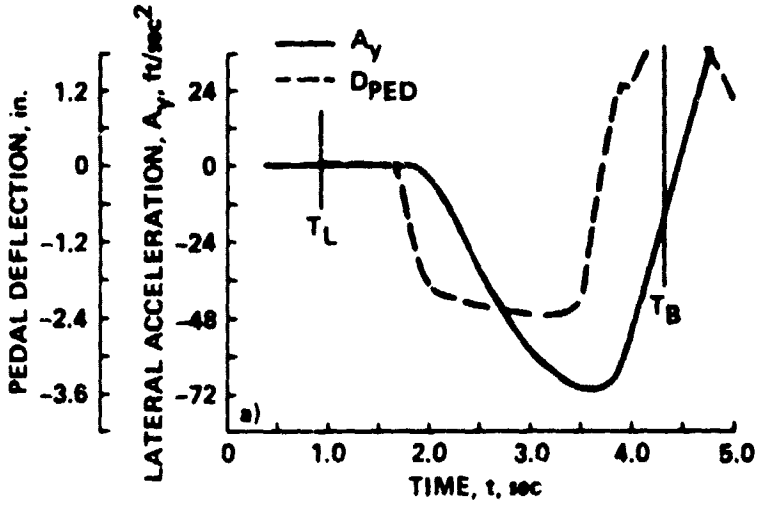

(a) $\zeta = 0.7$, $\omega_n = 2$, $\omega_b = 2.02$.

Figure 24.- Effect of bandwidth on the time history of the lateral acceleration response to pedal input, $\omega_b = 2.0$.

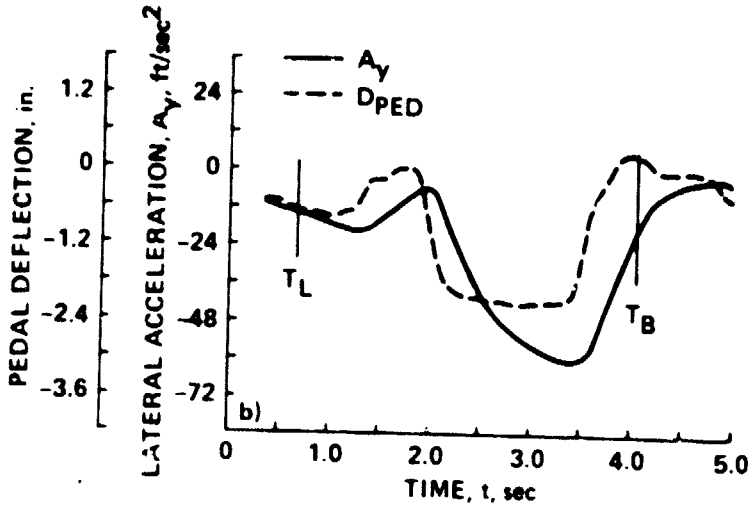

(b) $\zeta = 2.0$, $\omega_n = 8$, $\omega_b = 2.13$.

Figure 24.- Concluded.

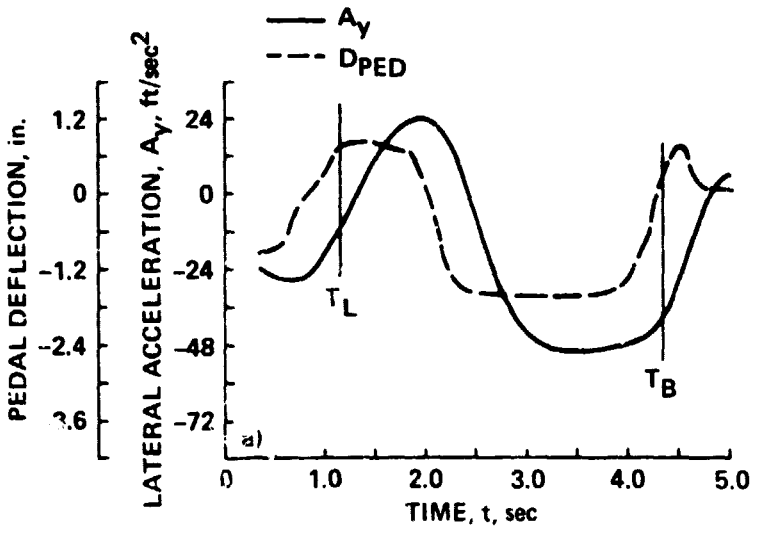

(a) $\zeta = 0.7$, $\omega_n = 3$, $\omega_b = 3.03$.

Figure 25.- Effect of bandwidth on the time history of the lateral acceleration response to pedal input, $\omega_b \approx 3.0$.

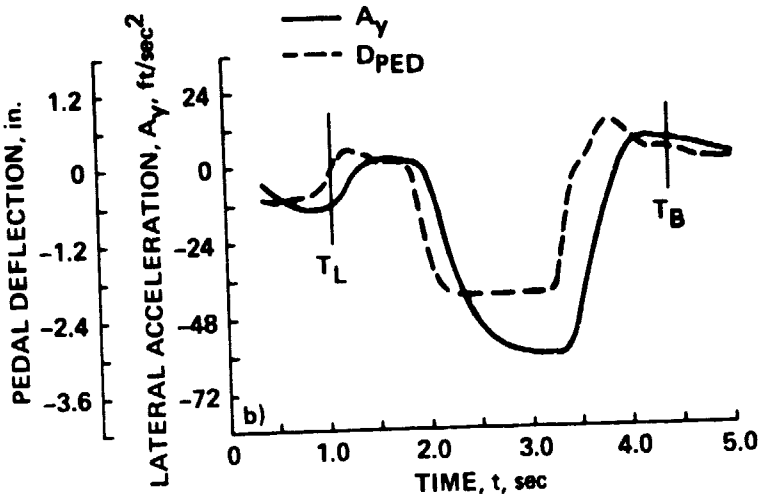

(b) $\zeta = 2.0$, $\omega_n = 12$, $\omega_b = 3.20$.

Figu ? 25.- Concluded.

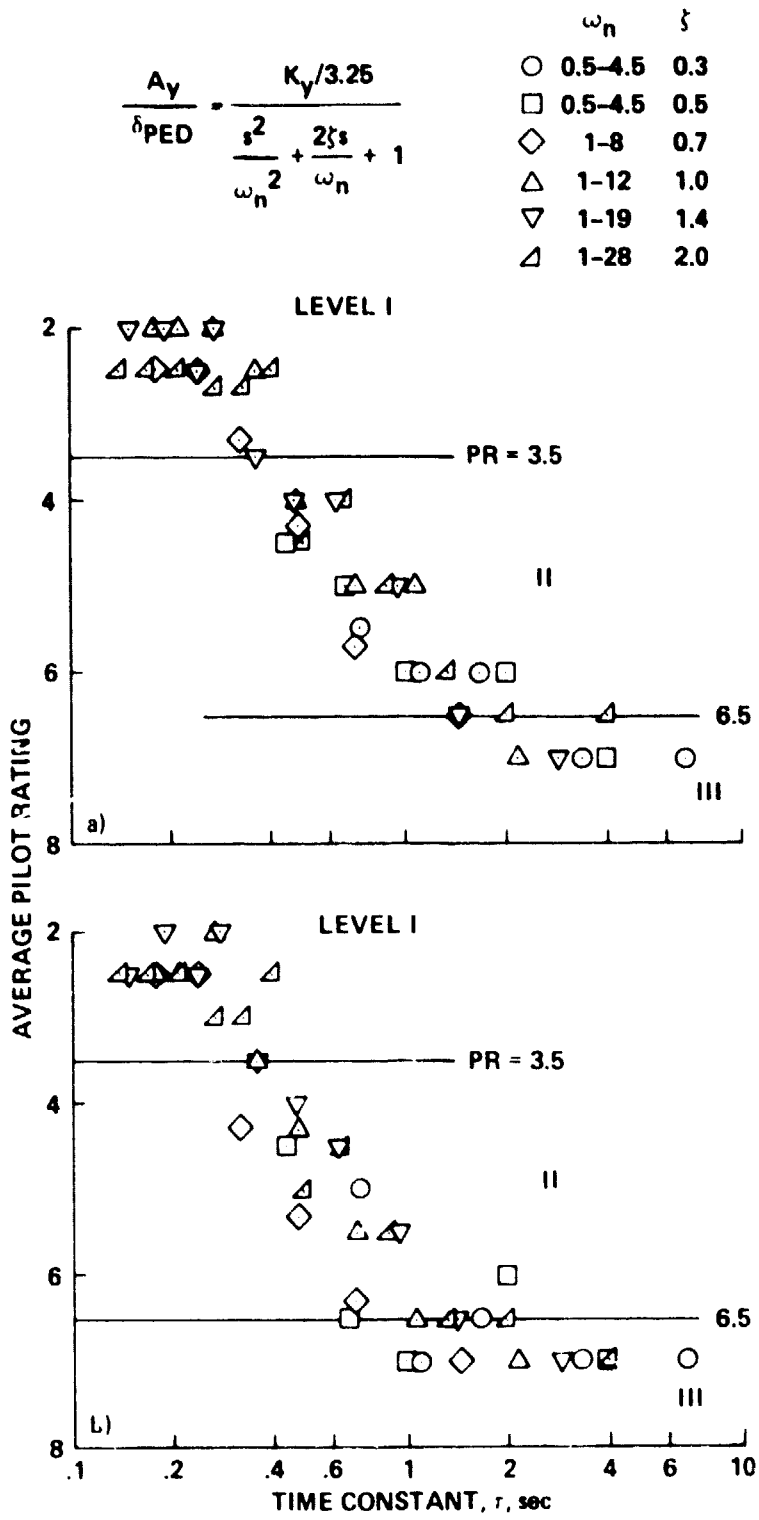

(a) Fine task.

(b) Coarse task.

Figure 26.- Effect of response time constant on pilot rating, Pilot A.

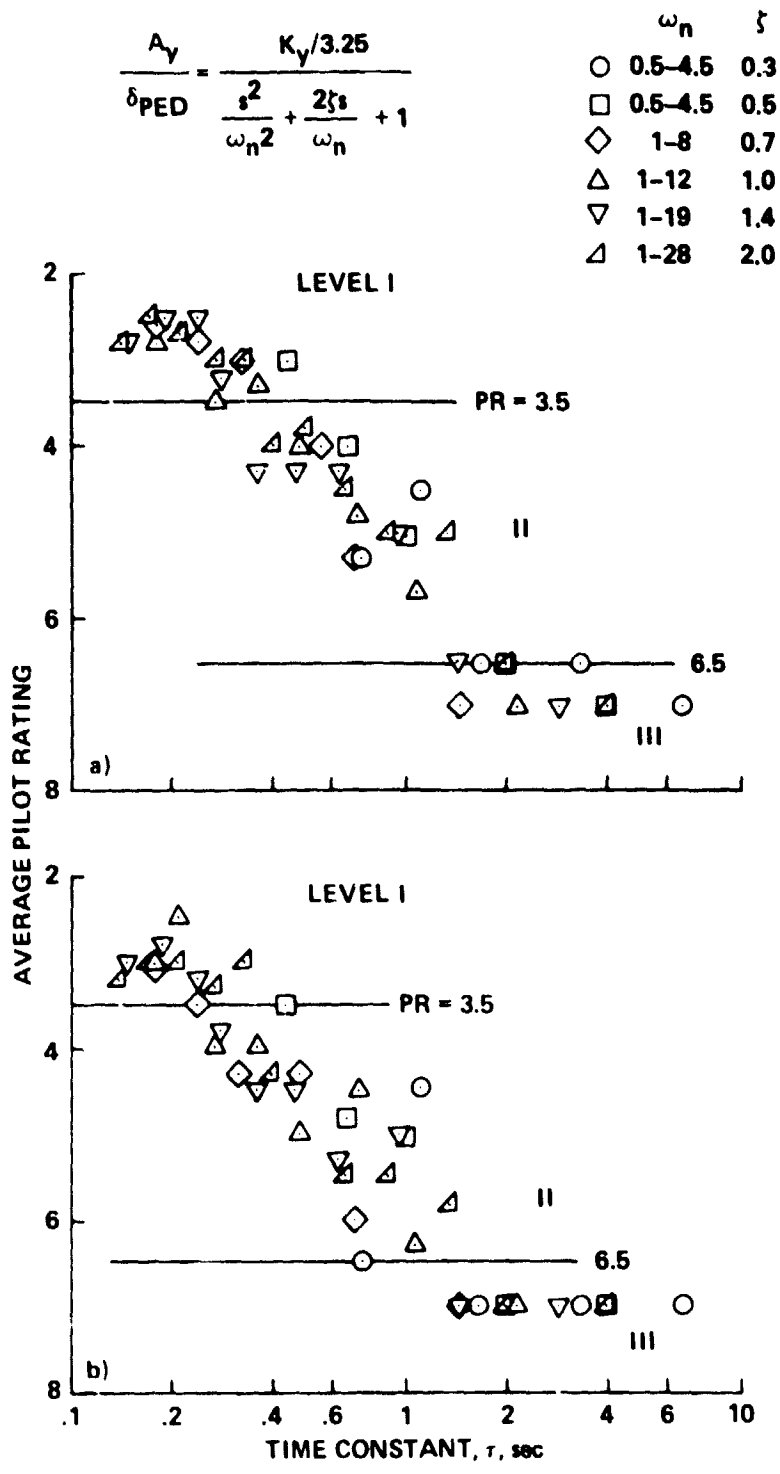

(a) Fine task.

(b) Coarse task.

Figure 27.- Effect of response time constant on pilot rating, Pilot B.

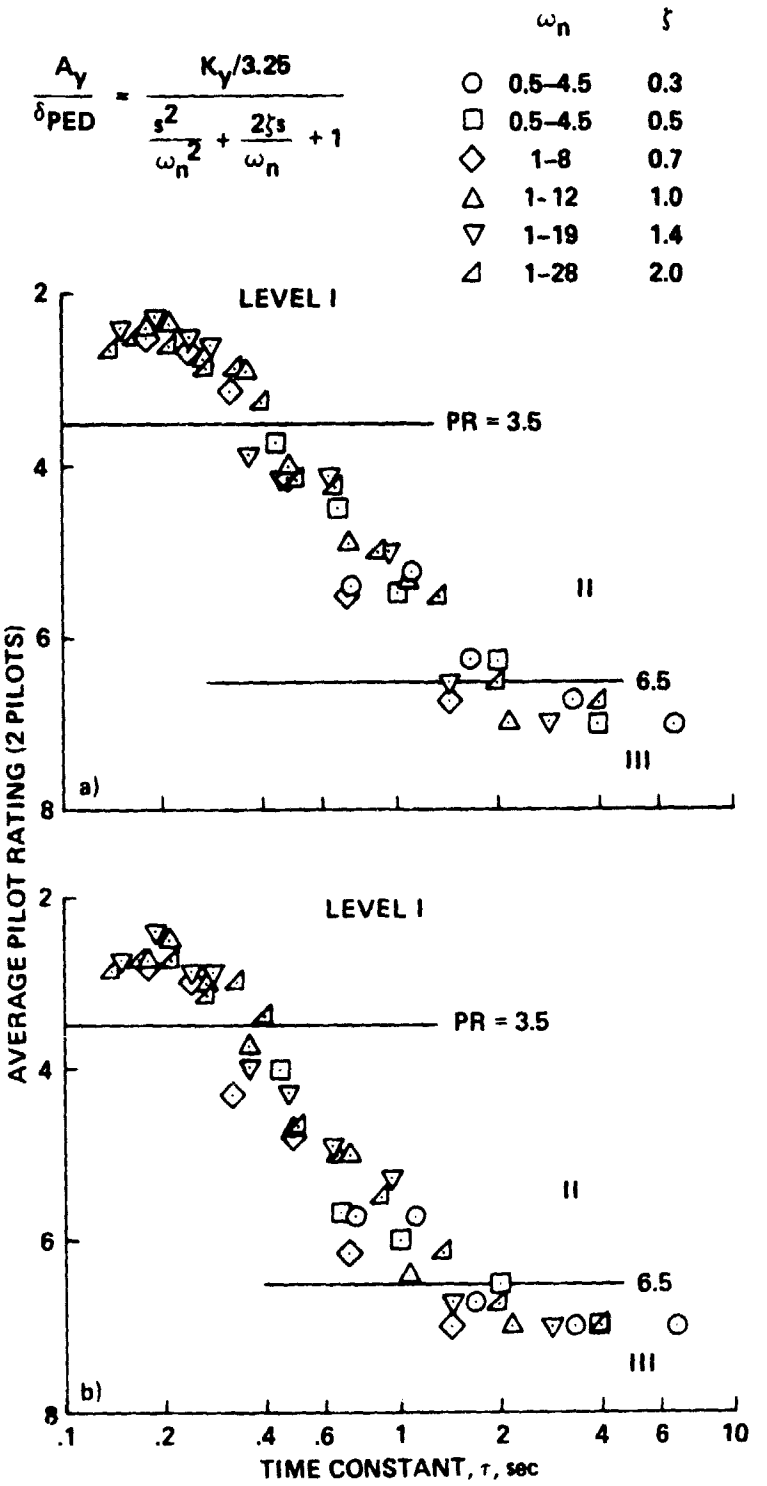

(a) Fine task.

(b) Coarse task.

Figure 28.- Effect of response time constant on pilot rating, Pilots A and B.

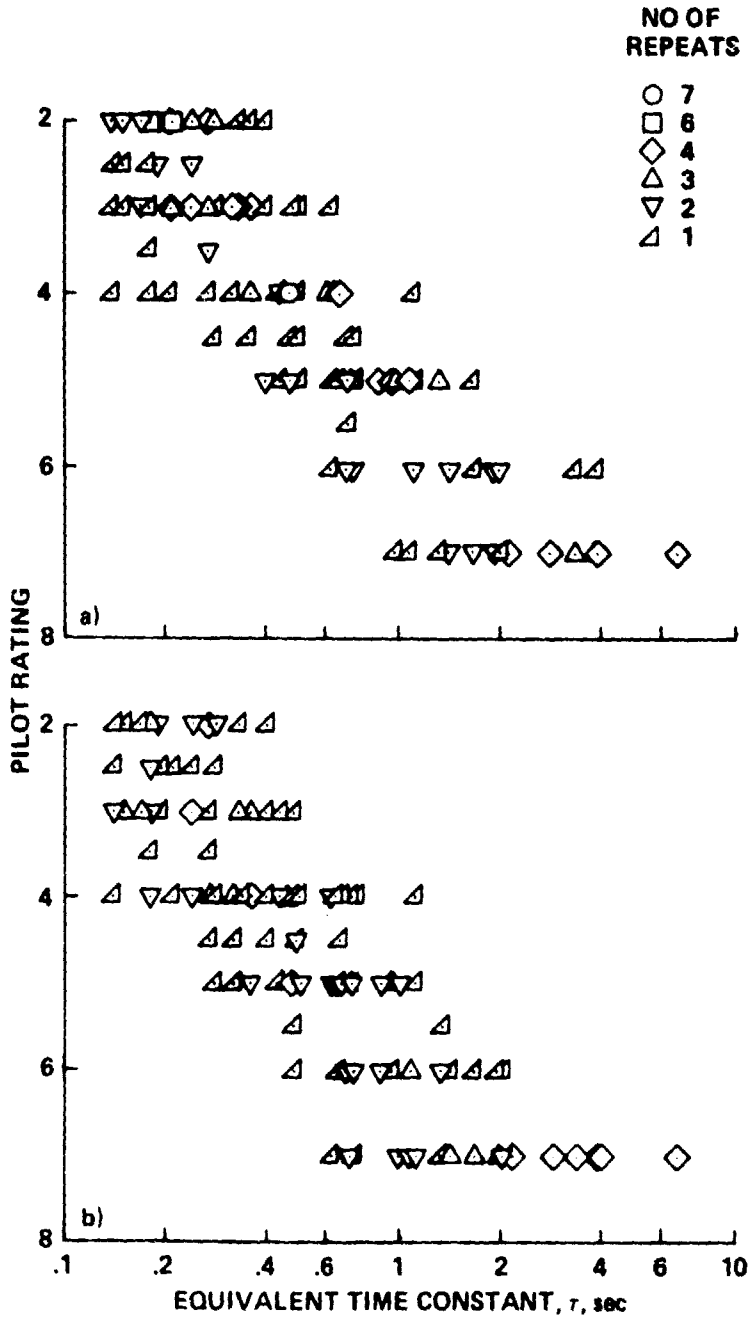

(a) Fine task.

(b) Coarse task.

Figure 29.- Effect of equivalent time constant on the distribution of the individual pilot rating for each pilot.

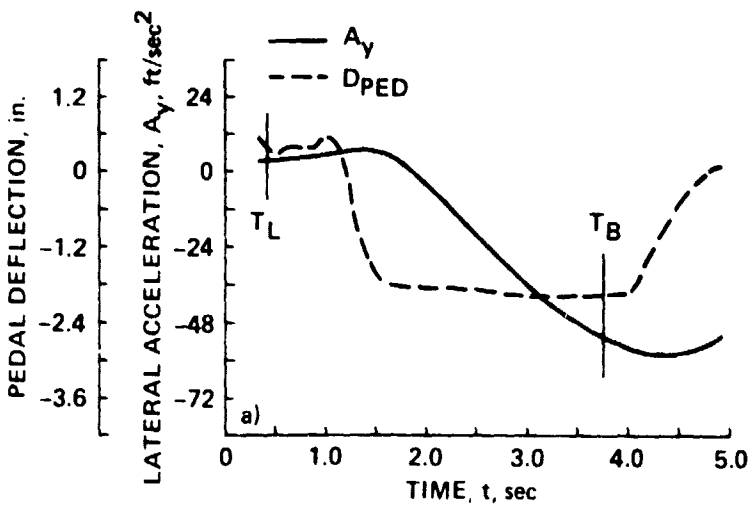

(a) τ = 1.43, ω_n = 1.0.

Figure 30.- Effect of equivalent time constant (τ) on the time history of the lateral acceleration response to pedal input, ζ = 0.7.

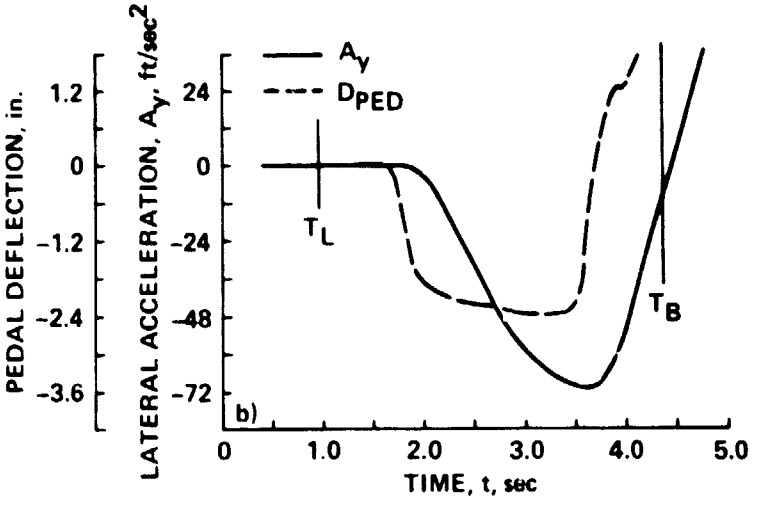

(b) $\tau = 0.71$, $\omega_n = 2.0$.

Figure 30.- Continued.

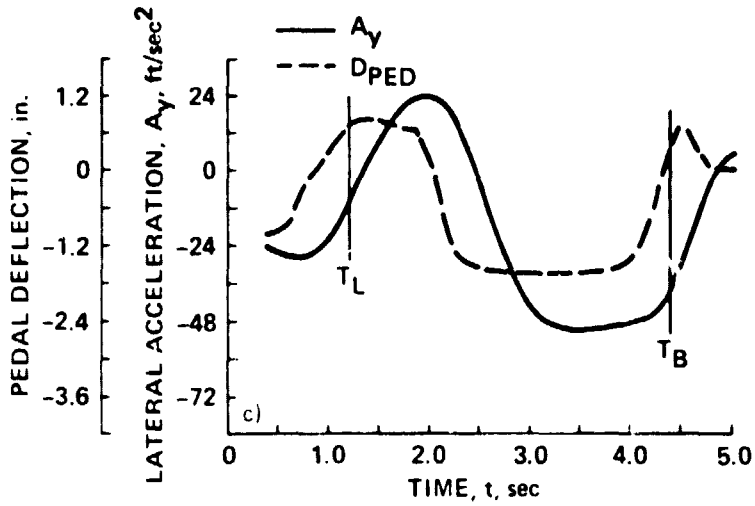

(c) τ = 0.48, ω_n = 3.0.

Figure 30.- Continued.

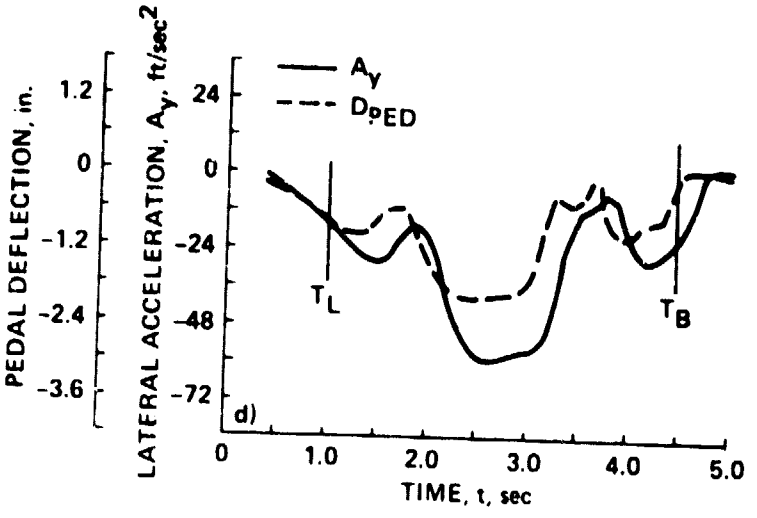

(d) $\tau = 0.18$, $\omega_n = 8.0$.

Figure 30.- Concluded.

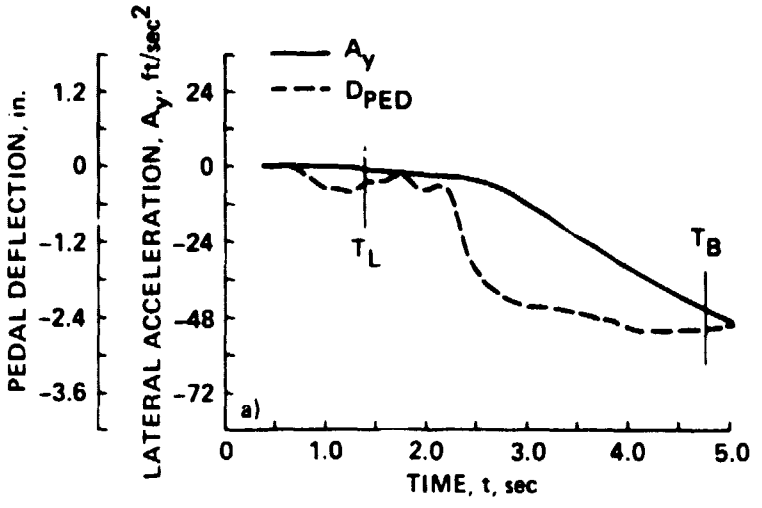

(a) $\tau = 2.84$, $\omega_n = 1.0$.

Figure 31.- Effect of equivalent time constant on the time history of the lateral acceleration response to pedal input, $\zeta = 1.4$.

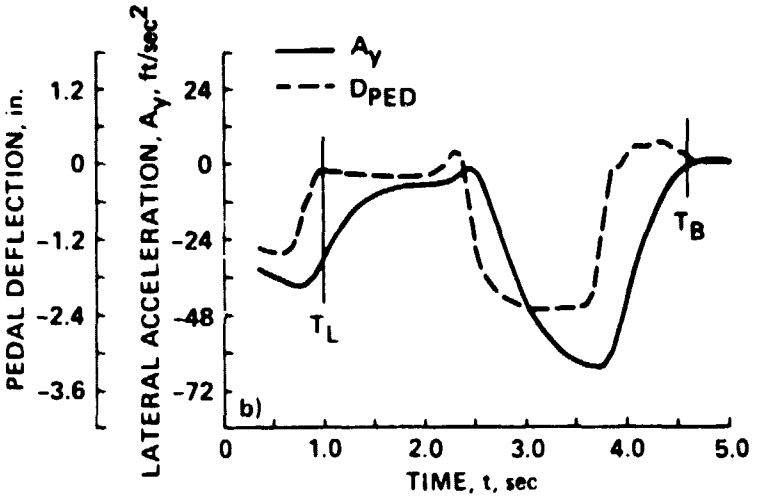

(b) $\tau = 0.47$, $\omega_n = 6.0$.

Figure 31.- Continued.

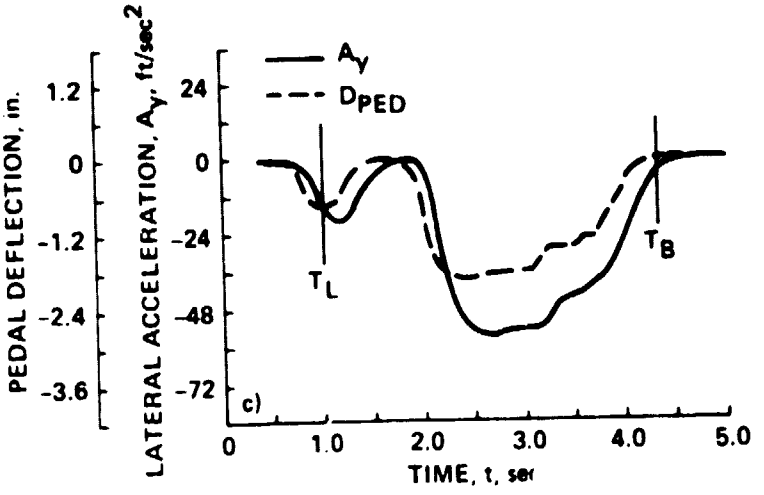

(c) $\tau = 0.15$, $\omega_n = 19.0$.

Figure 31.- Concluded.

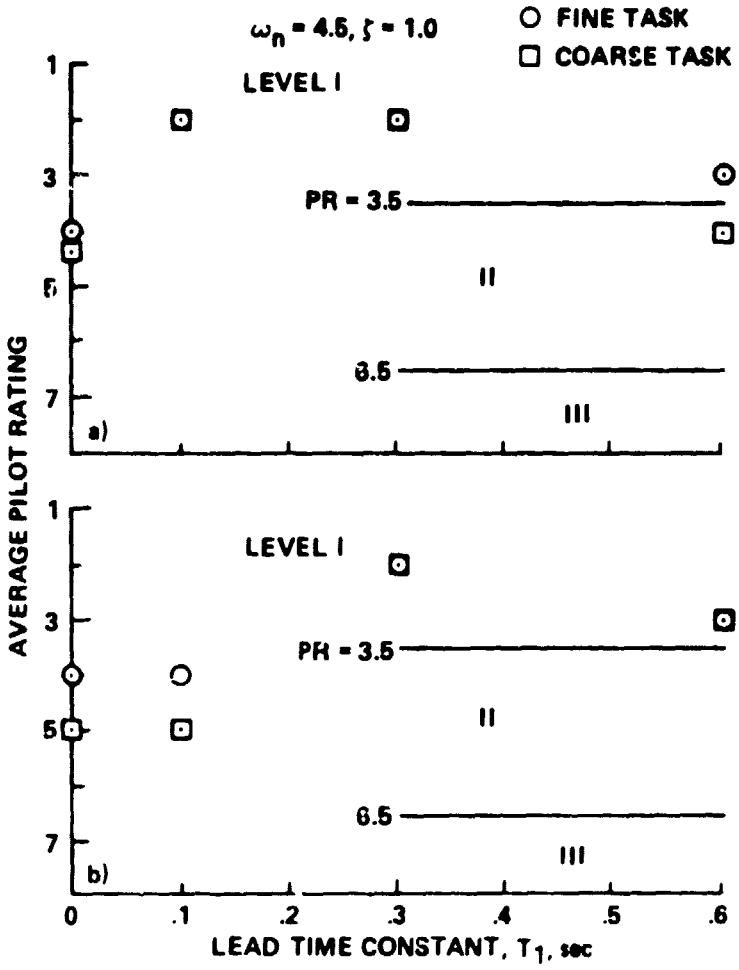

(a) Pilot A.

(b) Pilot B.

Figure 32.- Effect of lead time constant on pilot rating.

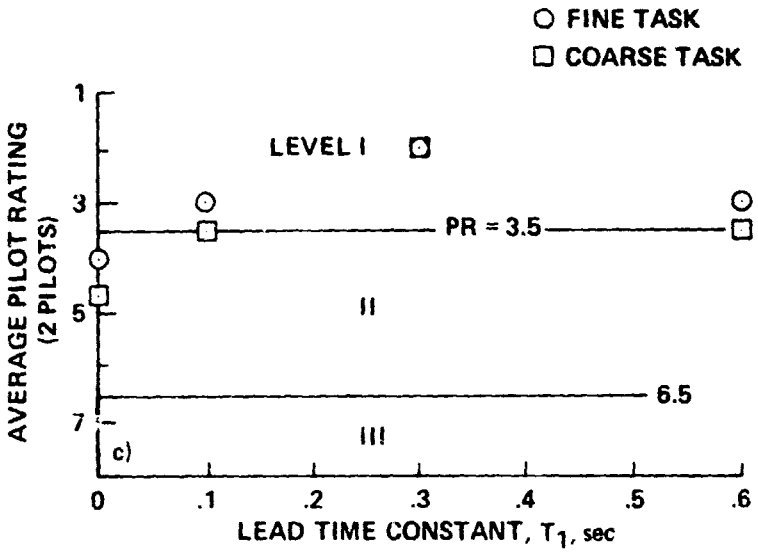

(c) Pilots A and B.

Figure 32.- Concluded.

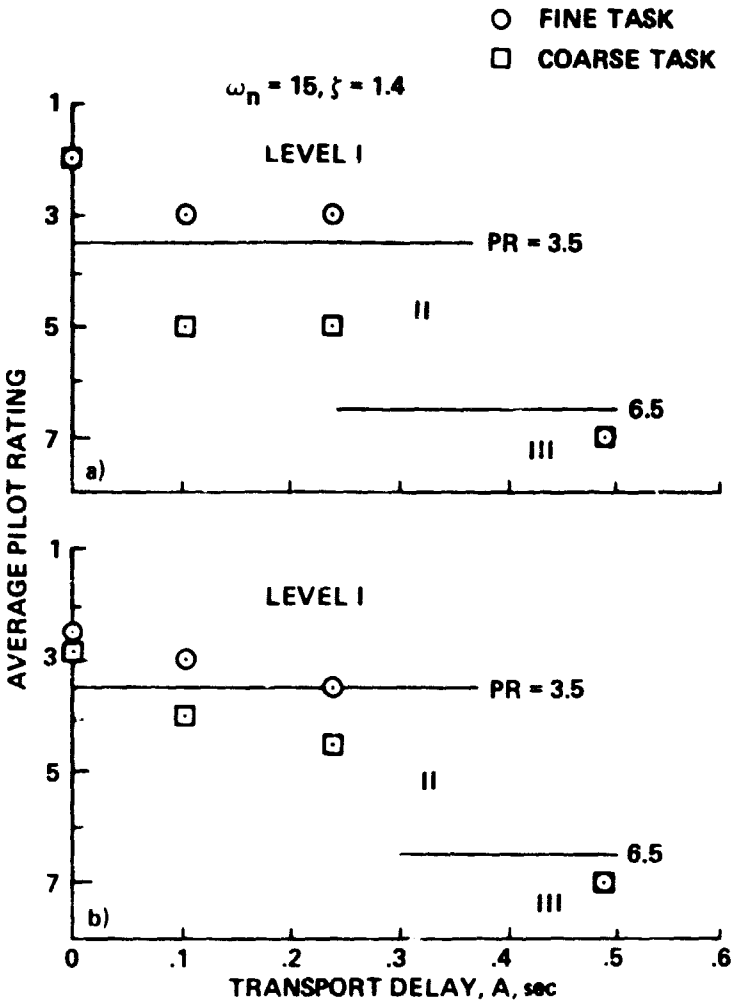

(a) Pilot A.

(b) Pilot B.

Figure 33.- Effect of transport delay on pilot rating.

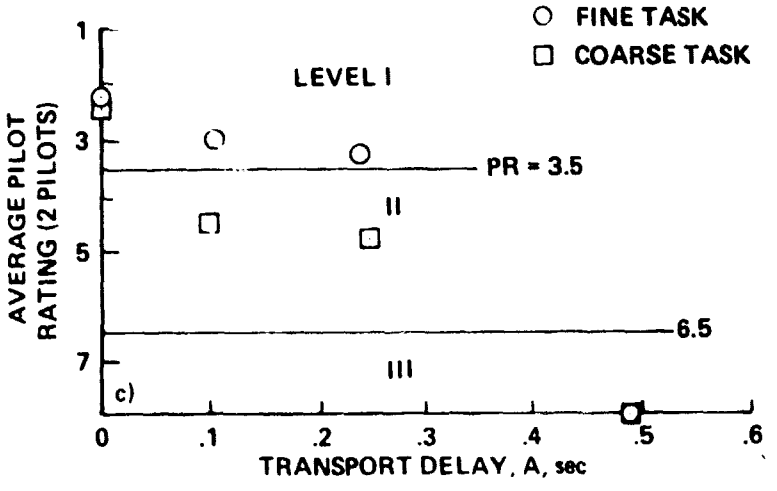

(c) Pilots A and B.

Figure 33.- Concluded.

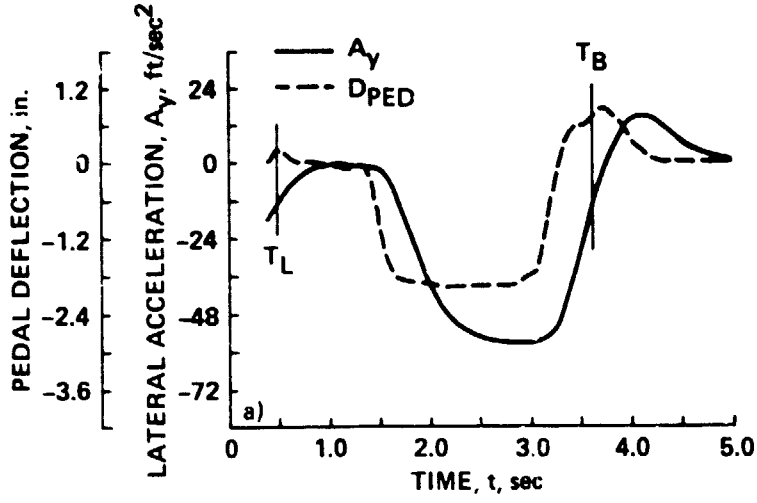

(a) $T_1 = 0$, $\tau = 0.48$.

Figure 34.- Effect of lead time constant on the time history of the lateral acceleration response to pedal input; $\zeta = 1.0$, $\omega_n = 4.5$.

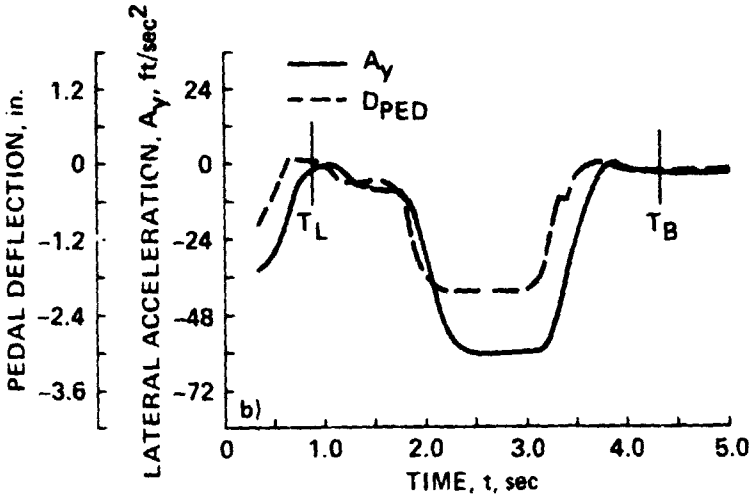

(b) $T_1 = 0.3$, $\tau = 0.16$.

Figure 34.- Concluded.

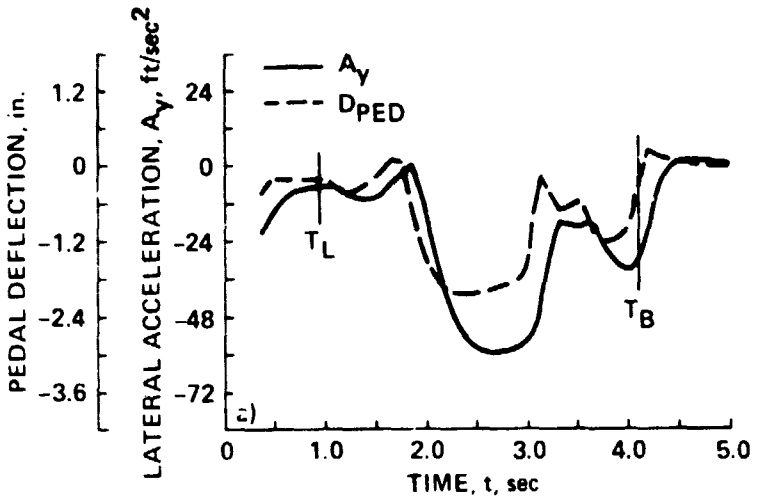

(a) A = 0, τ = 0.19.

Figure 35.- Effect of transport delay on the time history of the lateral acceleration response to pedal input; ζ = 1.4, ω_n = 15.

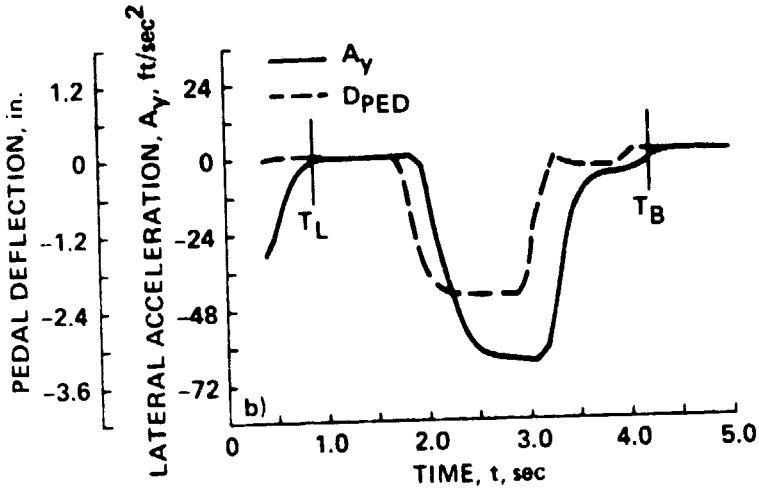

(b) A = 0.105, τ = 0.29.

Figure 35.- Continued.

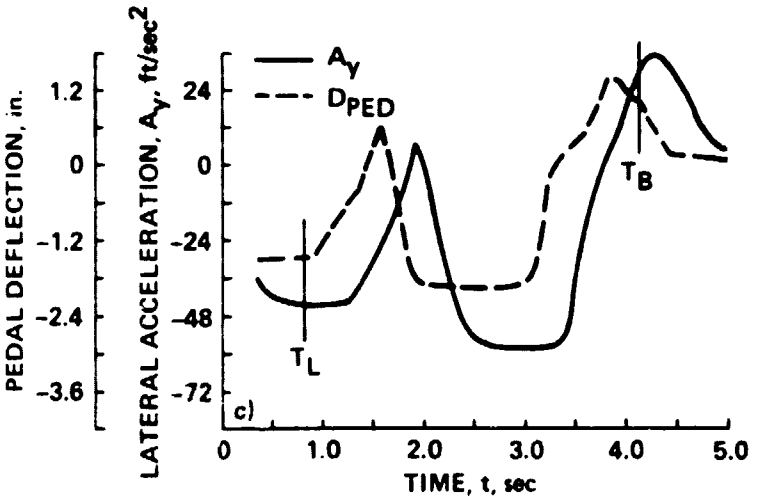

(c) A = 0.24, τ = 0.43.

Figure 35.- Concluded.

$$\frac{\Lambda_y}{\delta_{PED}} = \frac{(K_y/3.25)e^{-As}(T_1 s + 1)}{\frac{s^2}{\omega_n^2} + \frac{2\zeta s}{\omega_n} + 1}$$

	ω_n	ζ	T_1	A
△	4.5	1.0	0.1 - 0.6	–
▲	15	1.4	–	0.11 - 0.49

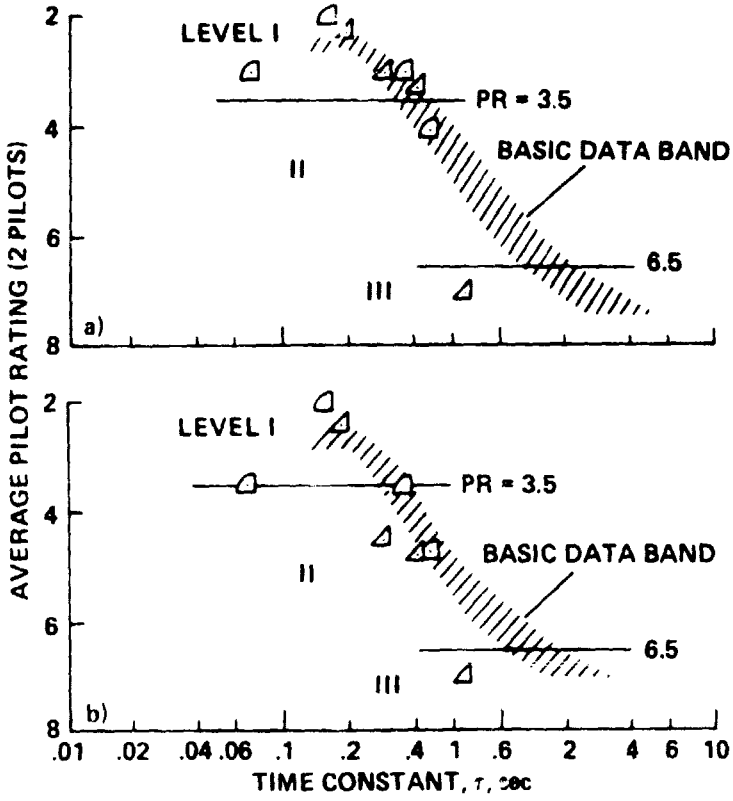

(a) Fine task.

(b) Coarse task.

Figure 36.- Effect of response time constant (including transport delay) on pilot rating.

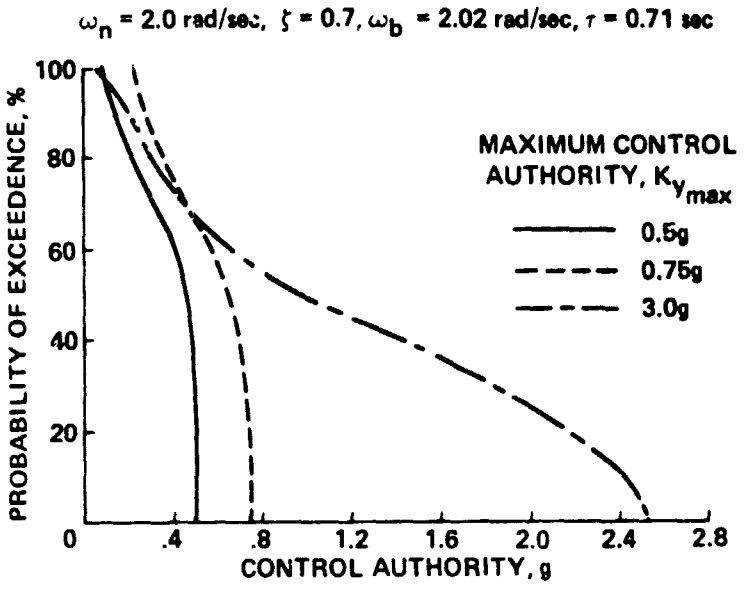

Figure 37.- Cumulative frequency distribution of commanded side acceleration, Pilot C.

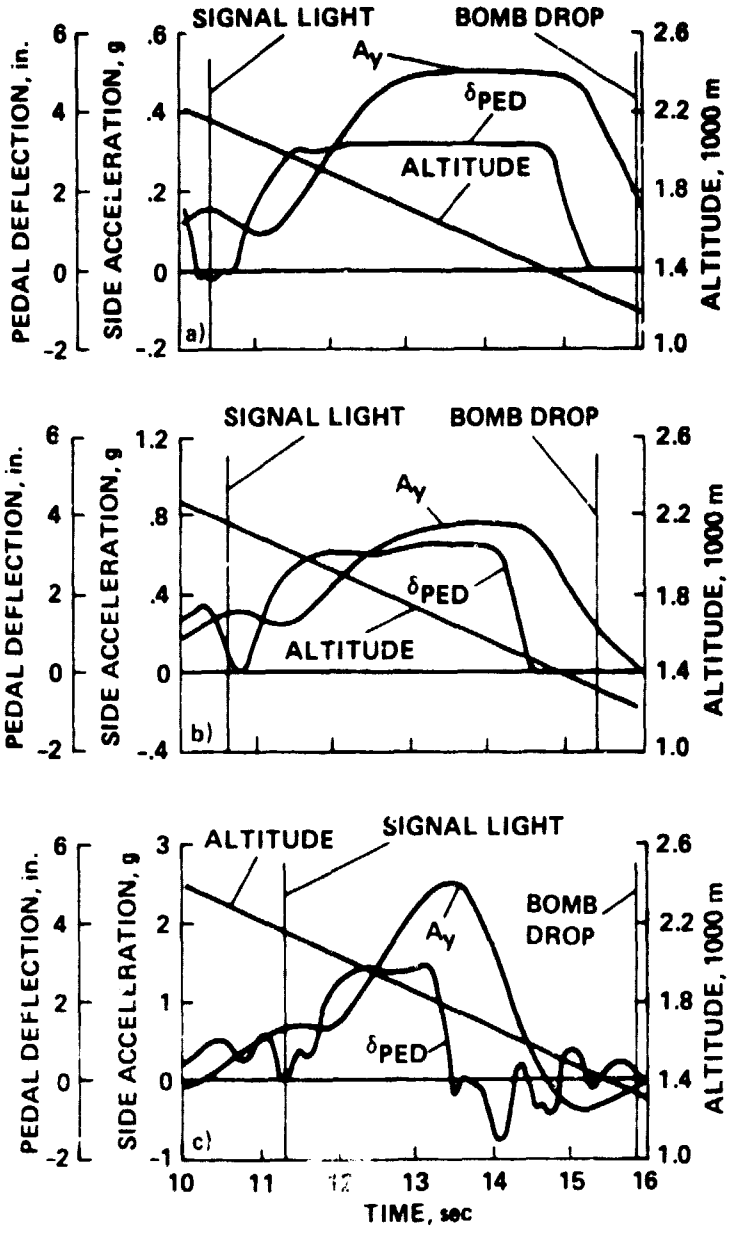

(a) $A_{y_{max}}$ = 0.5 g.

(b) $A_{y_{max}}$ = 0.75 g.

(c) $A_{y_{max}}$ = 3.0 g.

Figure 38.- Time history of wings-level-turn response to pedal input, Pilot C.

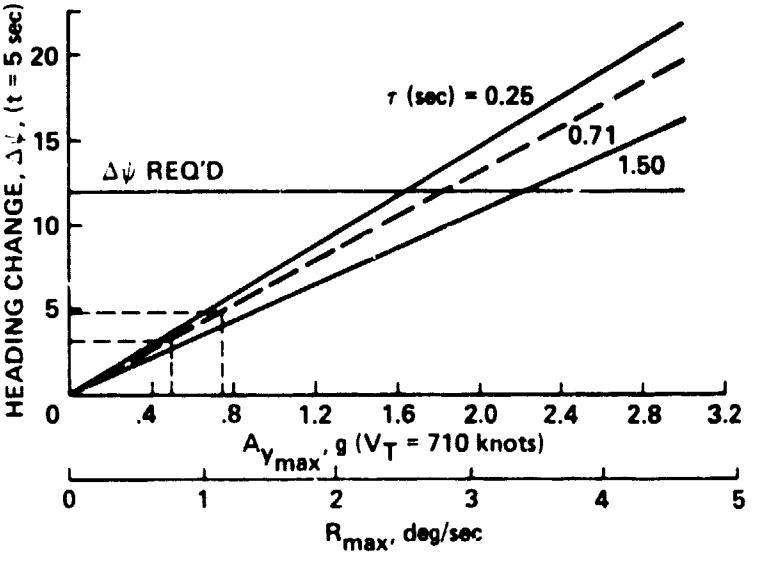

Figure 39.- Control power and time response required for particular heading change, $\Delta\psi$.